Organic & Biomolecular Chemistry c6ob01882c

1

Cyclodextrin-based facial amphiphiles: assessing the impact of the hydrophilic–lipophilic balance in the self-assembly, DNA complexation and gene delivery capabilities

Iris Pflueger, Coralie Charrat, Carmen Ortiz Mellet, José M. García Fernández, Christophe Di Giorgio* and Juan M. Benito*

Precise tailoring of cationic and lipophilic domains of cyclodextrin-based amphiphiles permits the control of the self-assembly capabilities and gene delivery efficiency of their aggregates.

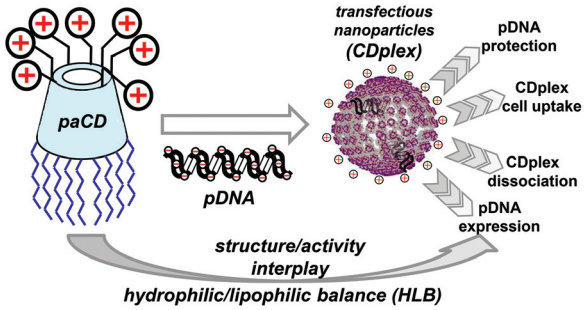

Please check this proof carefully. **Our staff will not read it in detail after you have returned it.**

Translation errors between word-processor files and typesetting systems can occur so the whole proof needs to be read. Please pay particular attention to: tabulated material; equations; numerical data; figures and graphics; and references. If you have not already indicated the corresponding author(s) please mark their name(s) with an asterisk. Please e-mail a list of corrections or the PDF with electronic notes attached – do not change the text within the PDF file or send a revised manuscript. Corrections at this stage should be minor and not involve extensive changes. All corrections must be sent at the same time.

Please bear in mind that minor layout improvements, e.g. in line breaking, table widths and graphic placement, are routinely applied to the final version.

We will publish articles on the web as soon as possible after receiving your corrections; **no late corrections will be made**.

Please return your **final** corrections, where possible within **48 hours** of receipt, by e-mail to: obc@rsc.org

Queries for the attention of the authors

Journal: **Organic & Biomolecular Chemistry**

Paper: **c6ob01882c**

Title: **Cyclodextrin-based facial amphiphiles: assessing the impact of the hydrophilic–lipophilic balance in the self-assembly, DNA complexation and gene delivery capabilities**

Editor's queries are marked like this [Q1, Q2, ...], and for your convenience line numbers are indicated like this [5, 10, 15, ...].

Please ensure that all queries are answered when returning your proof corrections so that publication of your article is not delayed.

Query Reference	Query	Remarks
Q1	For your information: You can cite this article before you receive notification of the page numbers by using the following format: (authors), Org. Biomol. Chem., (year), DOI: 10.1039/c6ob01882c.	
Q2	Please carefully check the spelling of all author names. This is important for the correct indexing and future citation of your article. No late corrections can be made.	
Q3	Do you wish to add an e-mail address for the corresponding author? If so, please supply the e-mail address.	
Q4	It is not clear what is meant by 'unforeseen' in 'unforeseen prospects'. I have changed it to 'potential prospects'. Is this what is meant?	
Q5	I have changed 'pretended effect' to 'projected effect'. Is this what is meant?	

Organic & Biomolecular Chemistry

PAPER

Cyclodextrin-based facial amphiphiles: assessing the impact of the hydrophilic–lipophilic balance in the self-assembly, DNA complexation and gene delivery capabilities†

Cite this: DOI: 10.1039/c6ob01882c

Iris Pflueger,[a] Coralie Charrat,[b] Carmen Ortiz Mellet,[c] José M. García Fernández,[a] Christophe Di Giorgio*[b] and Juan M. Benito*[a]

Received 26th August 2016,
Accepted 22nd September 2016

DOI: 10.1039/c6ob01882c

www.rsc.org/obc

Exhaustive structure–efficacy relationship studies on nonviral gene delivery systems are often hampered by the ill-defined or polydisperse nature of the formulations. Facial amphiphiles based on rigid cage-type molecular scaffolds offer unique possibilities towards these studies. Taking advantage of regioselective functionalization schemes, we have synthesized a library of cationic cyclodextrin (CD) derivatives combining a range of hydrophilic and lipophilic domains. We have scrutinized how the hydrophilic–lipophilic balance (HLB) around the CD scaffold determines their self-assembly capabilities and the DNA binding and release abilities of the corresponding CD : DNA nanocomplexes (CDplexes). These features have been ultimately correlated with their capabilities to deliver a reporter luciferase-encoding pDNA into COS-7 cells. The ensemble of results demonstrates that fine tuning of the HLB is critical to induce compaction of DNA by the CD-based facial amphiphiles into transfection-productive CDplexes.

Introduction

In vivo gene therapy has emerged as a fascinating therapeutic paradigm. The possibility to interfere with virtually any cellular metabolic process by specifically up- or down-regulating protein expression with exogenous nucleic acids holds potential prospects for the treatment of both, inherited or acquired diseases. Notwithstanding, its clinical impact is yet scarce as a consequence of the poor bioavailability of gene material and the biological hurdles impairing their efficient delivery to the therapeutic targets.[1–3] Nucleic acids are highly negatively charged molecules with low membrane permeability and metabolical stability. Their therapeutic use requires the development of purpose-conceived delivery systems, which remains so far a largely unmet challenge.[4] Transfection is a multistep process, involving among others nucleic acid condensation and protection from extra and intracellular media, cellular uptake, endosome escape, organelle targeting and cargo release; inefficiencies at any stage result in a dramatic decrease in its pretended effect.[5–7] Research efforts on nonviral gene vectors have intensified in the last two decades, seeking at improving the loading capacity, safety, and functional tunability to overcome the various biological barriers.[3,8–11] The ability to form stable nanocomplexes under physiological conditions, providing protection of the gene material from the action of nucleases, is a key aspect that has to be taken into consideration when designing an efficient gene carrier.[12,13] Yet, this self-assembly process must be reversible, since upon arrival into the intracellular medium the nucleic acid must be released; it becomes a liability for carriers to bind their cargo too tight, as overbinding impairs access to the translational machinery. Indeed, releasing inefficiencies are among the greatest obstacles for non-viral gene delivery[14,15] and there is a clear consensus that a balance between protection and DNA release should be sought.[5,16,17] Tackling this key challenge has brought into focus the analysis of series of polymeric carriers to probe the influence of factors such as polymer size,[15,18] cationic density,[19] conformation,[20] hydrophilic–lipophilic balance (HLB),[21] or simultaneously several of them.[22,23]

Vector performance optimisation strategies will greatly benefit from accurate structure–activity relationship studies and chemical tailoring-compatible approaches.[24] However, the polydisperse or multicomponent nature of most formulations severely restrict these initiatives.[25] Alternatively, molecularly

[a]Instituto de Investigaciones Químicas (IIQ), CSIC - Universidad de Sevilla, Américo Vespucio 49, E-41092 Sevilla, Spain
[b]Institut de Chimie Nice, UMR 7272, Université de Nice Sophia Antipolis, CNRS, 28, Avenue de Valrose, F-06108 Nice, France
[c]Departamento de Química Orgánica, Facultad de Química, Universidad de Sevilla, Profesor García González 1, E-41012 Sevilla, Spain

†Electronic supplementary information (ESI) available: Experimental details for nanoparticle formulation, biophysical characterization and biological evaluation, and copies of the NMR (^{1}H and ^{13}C) and ESI-MS spectra for all new compounds. See DOI: 10.1039/c6ob01882c

well-defined entities endowed with facial amphiphilicity based on rigid cage-type scaffolds,[26] such as fullerenes,[27] calixarenes,[28,29] pillarenes,[30] cyclopeptides,[31] or cyclooligosaccharides,[32] offer unprecedented opportunities in this regard. Among them, cationic cyclodextrin (CD)-based molecular gene vectors have gained a prominent position. CDs display a large number of hydroxyl groups with a well-defined spatial orientation that can be derivatized by synthetic means with relative ease. This feature offers virtually unlimited possibilities for functional tailoring of the CD core, which, together with their inherent biocompatibility and commercial availability, probably accounts for their profuse exploitation in the field.[32] Polycationic amphiphilic CDs (paCDs) readily promote nucleic acid condensation into stable nanometric particles (CDplexes) that mediate relevant expression levels of reporter and therapeutic genes in a variety of cell lines both *in vitro*[33,34] and *in vivo*.[35,36] CDplex formation is presumed to proceed through a two-step process involving (i) electrostatic-driven complexation of the DNA template of individual paCD entities along the polyphosphate chain; and (ii) hydrophobic-driven dehydration and compaction into nanocomplexes in which quasi-parallel nucleic acid segments are bridged by paCD bilayers (Fig. 1). It has been proposed that the balance between the cationic charge density in the hydrophilic rim and the hydrophobicity of the opposite face in the paCD structure governs this hierarchical assembly process, probably by controlling the reversible formation of the multilayer assembly.[37] Even though the notion of the HLB remains qualitative, studies on the lipophilization of pre-existing cationic carriers have revealed relevant performance improvements.[38] Interestingly, recent results[39] have shown that nanocomplexation of nucleic acids by non-amphiphilic cationic CDs can be elicited by promoting their supramolecular arrangement into dimeric species emulating the basic components of lipid-like bilayers.

In this contribution we aim at providing a deeper insight into the molecular basis underlining the efficacy of facial amphiphiles as gene vectors by pinpointing how HLB controls hierarchical paCD self-assembly around DNA strands and the stability of the corresponding CDplexes. First, a library of βCD derivatives combining an array of cationic and lipophilic elements in segregated domains was built (Chart 1). Next, the kinetics and dynamics of the paCD : DNA interactions involved in CDplex formation and dissociation in aqueous media were scrutinized for each library member individually. Finally, the pDNA-transfecting capabilities *in cellulo* have been assessed and critically correlated with the molecular and supramolecular features. Collectively the data point out that, despite all cationic CDs efficiently complexing DNA, gene transfer capabilities critically depend on a delicate balance between the factors influencing reversible CDplex assembly–disassembly among which the HLB plays a central role.

Results and discussion

Library design and synthesis

For the goals of this work, we have taken advantage of a previously described strategy for face-selective functionalization of native CDs permitting the construction of precise functional group displays.[33,40] The strategy consists of the regioselective cysteaminylation of the primary hydroxyl rim, followed by exhaustive acylation of the secondary ones (Scheme 1). The hydrophilic (cationic) domain can be further tailored by using a click-type thiourea-forming reaction.[41] For each multihead cationic cluster architecture, the length of the hydrophobic tails at the opposite face can be varied preserving full homogeneity and a C_7-symmetrical arrangement by DMAP-promoted acylation with different acyl anhydrides, overall keeping a limited synthetic cost. Two series of cationic CDs featuring 7 or 21 potentially cationizable amino groups on the primary CD rim, respectively (Chart 1, **7**- and **21**-series in the left and right panels) were thus prepared. The members of each series are furnished at their secondary rim with 14 acyl groups of varied length (from acetyl to hexanoyl). Each series was completed with the corresponding non-amphiphilic CD derivative keeping the secondary hydroxyls unmodified ($\mathbf{7_H}$ and $\mathbf{21_H}$). In brief, synthesis started from the common precursor per-(C-6)-bromo βCD,[42] which was transformed into the cysteaminylated derivative **1** [33] upon treatment with Boc-protected 2-aminoethanethiol. Compound **1** was then subjected to acylation of the

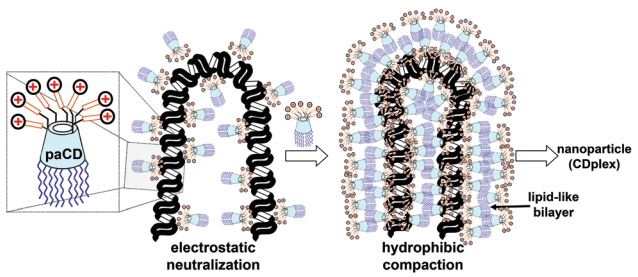

Fig. 1 Schematic representation of the stepwise process leading to CDplex formation, consisting on (i) the initial electrostatic interaction of paCDs with the negatively-charged nucleic acid, and (ii) the latter hydrophobic compaction forming a bilayered paCD shell around the nucleic acid template.

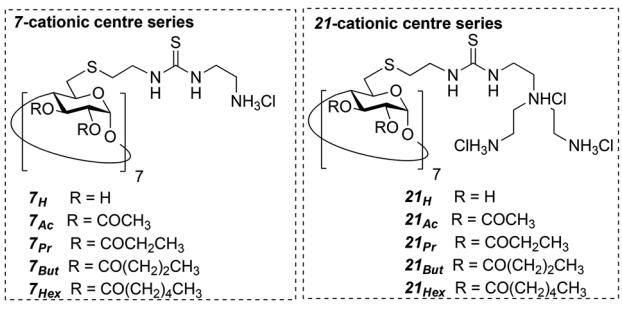

Chart 1 Structure of **7**- and **21**-cationic CD series with indication of their structure-correlated notation (**7** or **21** refer to the number of potentially protonatable amines at the primary rim of the CD scaffold, while subscripts indicate the functionalization at the secondary rim).

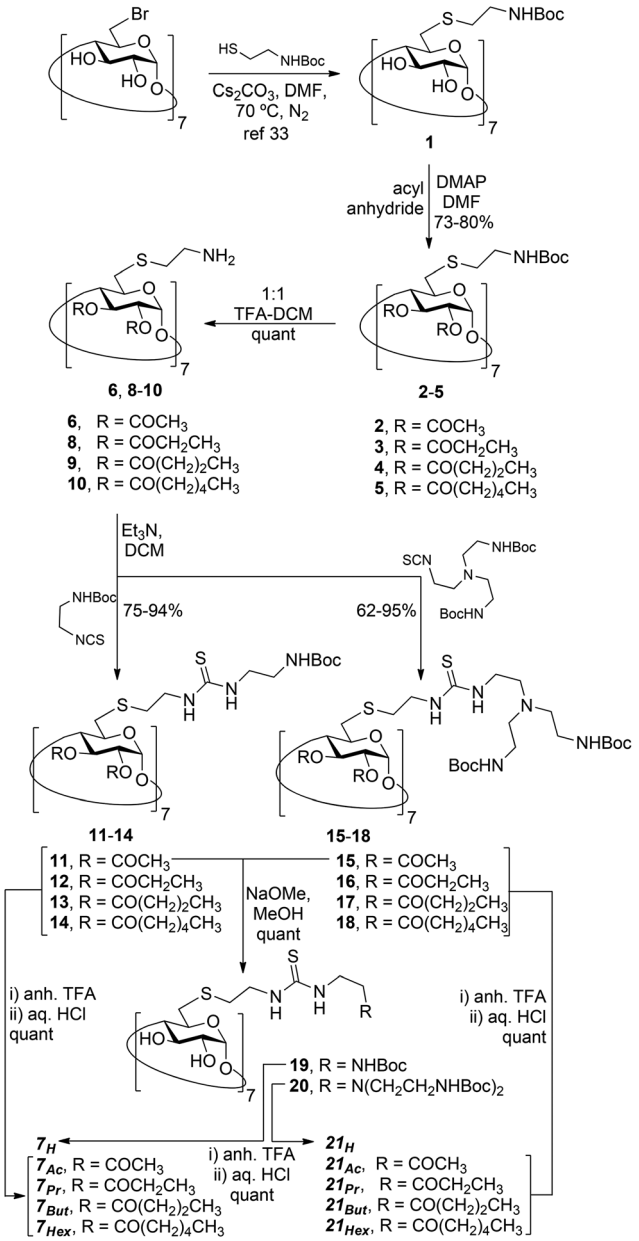

Scheme 1 Synthesis of paCDs in the **7**- and **21**-series. For a more intuitive structural correlation, notations combine the number of protonable amine groups (7 or 21) with an acronym of the acyl groups at the secondary rim.

secondary hydroxyls to efficiently yield derivatives **2–5** in 73–80% yield (Scheme 1). TFA-promoted Boc cleavage, followed by multi-thiourea coupling of the resulting heptaamines **6** and **8–10** with 2-(*tert*-butoxycarbonylamino)ethyl isothiocyanate,[43] afforded the Boc-protected adducts **11–14** (**7**-series) in 75–94% overall yield after column chromatography purification. Alternatively, coupling the cysteaminyl derivatives **6–10** to 2-[bis(2-(*tert*-butoxycarbonylamino)ethyl)amino]ethyl isothiocyanate[33] efficiently furnished the Boc-protected dendritic derivatives **15–18** (**21**-series) in 62–95% overall yield (Scheme 1). The non-amphiphilic derivatives **19** and **20** were prepared from the corresponding acetylated adducts (**11** and **15**, respectively) by Zemplén transesterification in methanolic NaOMe (Scheme 1).

Treatment of the Boc-protected thiourea adducts with concentrated TFA (either in water or DCM) has been shown to quantitatively produce the corresponding cationic amphiphiles.[33,44] However, this protocol concomitantly produced extensive ester hydrolysis in substrates with the shorter acyl chains (acetyl and propanoyl, see ESI, Fig. S29†). The use of anhydrous TFA at 0 °C and short reaction times, followed by freeze-drying from aqueous HCl prevented this undesired side-reaction and furnished the target paCDs quantitatively as their hydrochloride salts (Scheme 1 and Chart 1). The purity and homogeneity of each library member was assessed by NMR, ESI-MS, and combustion analysis.

The optimal conditions to obtain a satisfactory ^{1}H NMR spectral resolution for each paCD derivative varied from case to case (see Experimental section) and were very much dependent on the solvent, pH and acquisition temperature. This probably reflects the disparate self-assembling capabilities of these facial amphiphiles as a function of their molecular structure. For instance, the very broad resonance signals exhibited by derivative $\mathbf{7_{Pr}}$ in D_2O-containing solution dramatically resolved in DMSO-d_6 (Fig. S30†), indicating the aggregating tendency in aqueous media. On the other hand, derivative $\mathbf{7_{Hex}}$ exhibited a complex spectrum at acidic pH that readily simplified upon neutralization (Fig. S31†), which was attributed to slow proton exchange between cationic head groups in an acidic environment even at relatively high temperatures (50 °C). As expected, non-amphiphilic CDs $\mathbf{7_H}$ and $\mathbf{21_H}$ did not exhibit this behavior.

DNA complexing abilities of cationic CDs

Study of CDplex formation by DLS. To analyze the influence of the HLB on nucleic acid complexing capabilities, the size and ζ-potential of paCD : DNA CDplexes were measured by dynamic light scattering (DLS), respectively. Due to the limited availability of the transfection plasmid, preliminary assessments were made at several N/P ratios using a commercial calf thymus DNA (ctDNA) as pDNA surrogate. None of the cationic CDs formed ordered aggregates in the absence of DNA when dispersed either in water or HEPES buffer. Rather polydisperse and unstable aggregate populations were obtained in most cases. In contrast, in the presence of ctDNA all candidates rendered rather homogenous nanocomplexes (60–90 nm, Fig. 2) at ionizable nitrogen/phosphate (N/P) ratios of 5 and 10, thus confirming the templating role of DNA in CDplex assembling (see Fig. S34†). Minor size and ζ-potential variations were observed between the two N/P ratios considered, suggesting that once DNA is fully complexed the excess of cationic CD plays a minor role in CDplex morphology. Particle size distribution analysis in the N/P 5–10 window indicates that single population of CDplexes are formed from most formulations, with narrow size distributions especially in the case of paCD derivatives equipped with the longer acyl chains (*e.g.* Fig. S34C†). CDplexes formulated at N/P ≤ 2 averaged larger

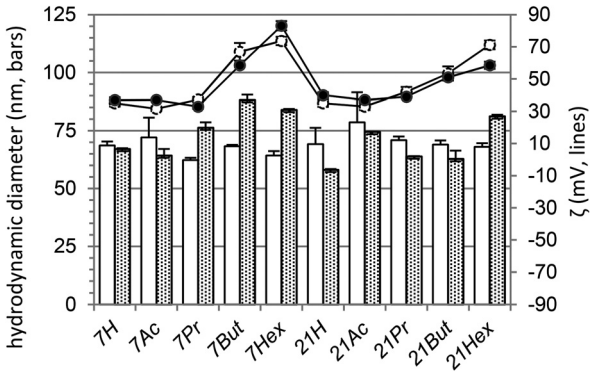

Fig. 2 Hydrodynamic diameter (bars, left axis) and ζ potential (circles, right axis) of CDplexes formulated at N/P 5 (empty bars and circles) and 10 (filled bars and circles).

particle sizes and polydispersities than the corresponding formulations at N/P 5 or 10 (data not shown), indicating suboptimal particle compaction and, probably, reduced stability. Transmission electron microscopy (TEM) and gel electrophoresis retardation experiments (*vide infra*) also support this hypothesis.

ζ-Potential values showed higher variability within each paCD series. Thus, the most hydrophilic derivatives ($\mathbf{7_H}$, $\mathbf{7_{Ac}}$, $\mathbf{7_{Pr}}$ and $\mathbf{21_H}$, $\mathbf{21_{Ac}}$, $\mathbf{21_{Pr}}$) featured mildly positive potentials in the 31.6–37.3 mV range, regardless of the N/P (5 or 10) or the nature of the cationic heads, whereas the most lipophilic CDs ($\mathbf{7_{But}}$, $\mathbf{7_{Hex}}$ and $\mathbf{21_{But}}$, $\mathbf{21_{Hex}}$) exhibited significantly higher ζ-potentials, in the 49–85 mV range.

Agarose gel electrophoresis retardation experiments. The above results were contrasted with agarose gel electrophoresis shift assays. CD : ctDNA complexes were formulated at different N/P ratios (0.5 to 20) and their electrophoretic mobility was compared to that of ctDNA alone. The accessibility of the nucleic acid material in the nanocomplexes was examined by staining with the intercalating agent GelRed™. As expected, all cationic CDs inhibit ctDNA migration, but remarkable differences in both the capacity to neutralize DNA and to protect it from GelRed™ intercalation as a function of the HLB is observed. The non-amphiphilic cationic CDs $\mathbf{7_H}$ and $\mathbf{21_H}$ are the most efficient at neutralizing ctDNA, although incomplete DNA protection from the media is observed even at the highest N/P ratio tested (Fig. 3, first row). Conversely, DNA retardation and protection against the intercalating agent gradually increased in parallel to the N/P ratio in the case of DNA : paCD formulations, the facial amphiphiles equipped with the longest hexanoyl chains $\mathbf{7_{Hex}}$ and $\mathbf{21_{Hex}}$ being the most efficient at both tasks. At a first glance, derivatives from the **7**-series seems to be superior to their **21**-series counterparts, which might be rationalized considering that a 3-fold higher molar concentration is required for the former to achieve identical N/P ratios. Except for $\mathbf{7_{But}}$ and $\mathbf{7_{Hex}}$, N/P values >2 are required to achieve complete DNA protection. Qualitatively similar results were obtained when replacing ctDNA by pDNA (data not shown).

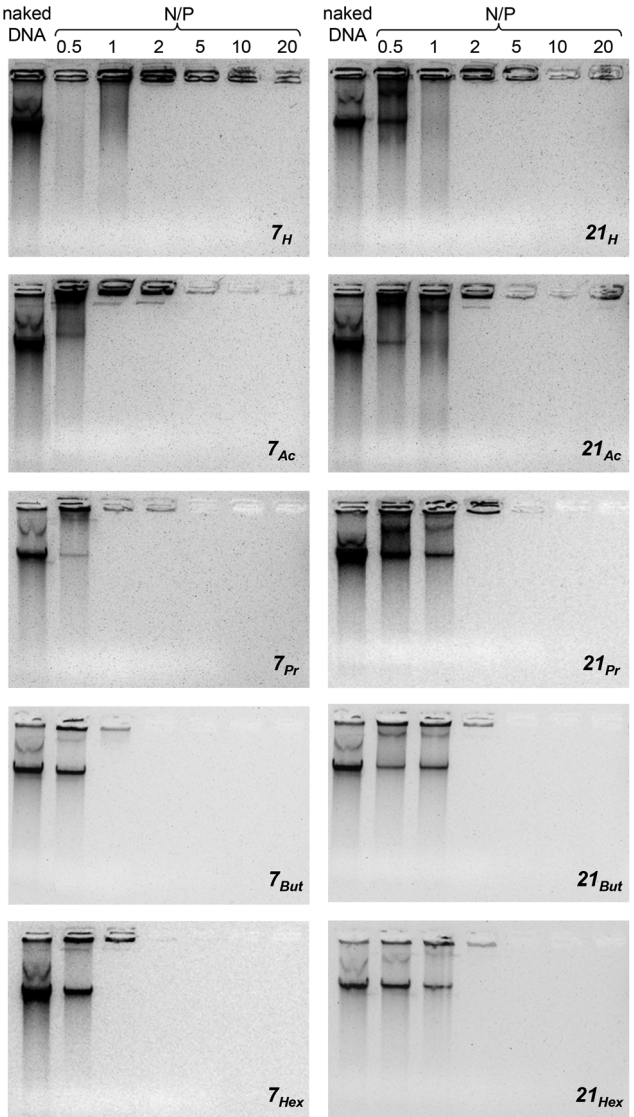

Fig. 3 ctDNA retardation and protection capacity of CDs (**7**-cationic CDs, left column; **21**-cationic CDs, right column) in agarose gel at different N/P ratios (0.5, 1, 2, 5, 10 and 20). Environmentally accessible nucleic acid is visualized by GelRed™ staining.

Transmission electron microscopy of CDplexes. The TEM micrographs of N/P 10 pDNA : paCD formulations evidenced significant differences on the self-assembly properties of the facial amphiphiles as a function of the HLB as well as on their ability to form mixed nanocomplexes where the condensed plasmid is isolated from the environment. The paCDs equipped with the shorter acetyl or propionyl chains (*e.g.* $\mathbf{7_{Ac}}$ and $\mathbf{21_{Pr}}$, Fig. 4A and B) tend to self-assemble into small nanoaggregates (10–20 nm diameter), previously unnoticed in DLS measurements. These particles are likely to interact electrostatically with pDNA molecules to form, initially, large (>200 nm) multiparticle : plasmid aggregates, as observed in Fig. 4A. Eventually, these aggregates can further collapse to afford multilamellar CDplexes, probably unimolecular in

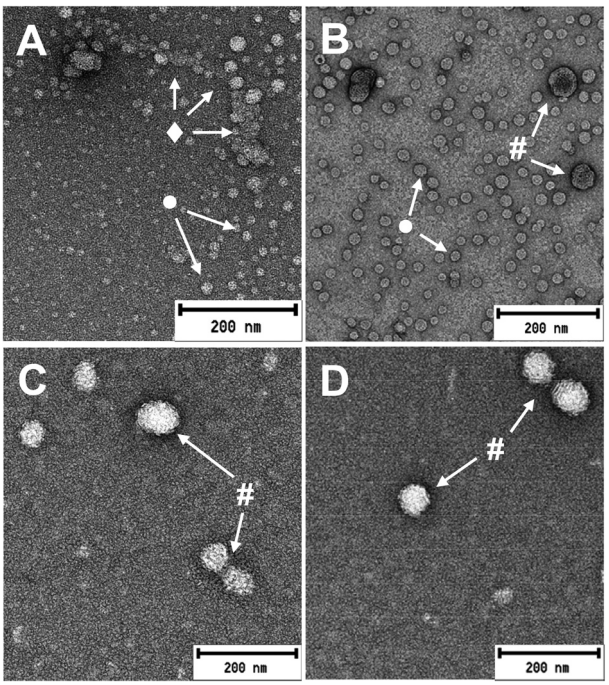

Fig. 4 TEM micrographs of CDplexes formulated at N/P 10 with (A) 7_{Ac}, (B) 21_{Pr}, 7_{But} (C) and (D) 21_{Hex} in the presence of pDNA. The symbols ●, ◆, and # indicate small (10–20 nm) CD vesicles, multivesicle : DNA aggregates, and CDplexes, respectively.

pDNA, in which paCD bilayers alternate with DNA segments. CDplexes and paCD vesicles coexist in these formulations and can be observed simultaneously in the TEM images. In sharp contrast, in the formulations prepared from butyroyl and hexanoyl paCD derivatives (*e.g.* 7_{But} and 21_{Hex}, respectively) only the collapsed well-defined CDplexes are observable, suggesting that the paCD in excess does not form stable self-assembled constructs (Fig. 4C and D). In summation, the ensemble of TEM data strongly suggests that in the first scenario the dynamic equilibrium underlining CDplex assembly–disassembly involves vesicular species, whereas in the second case it implies molecular entities. Shifting from one situation to the other drastically depends on the HLB, the transition occurring between paCDs bearing propanoyl and butanoyl chains at the secondary hydroxyls in the two series of facial amphiphiles here studied. The results evidence that, as far as concerning self-assembling abilities, the volume of the lipophilic cluster (determined by acyl chain length) is the decisive factor, as compared to the cationic density. It is reasonable to argue that breaking the paCD vesicles implies a certain energy penalty that renders CDplexes from acetylated and propanoylated paCDs less stable than the butanoylated and hexanoylated homologues, in agreement with the agarose gel retardation experiments above discussed.

DNA releasing abilities of CDplexes

Heparin competition experiments. A functional gene vector must not only condense and protect the gene material by forming nanocomplexes capable of crossing biological membranes, but also must deliver the nucleic acid cargo at the right spot. The steps leading to CDplex disassembly and DNA release are at least as important as those involved in DNA protection to the overall transfection process. Previous results indicated that facial amphiphilicity furnishes CDplexes with higher tolerance to saline stress[33] as compared to non-amphiphilic CD polycations, which readily dissociate at high ionic strength.[45] This is reasonable considering that the formation of the latter exclusively rely on electrostatic interactions, whereas in the case of paCDs a hydrophobic contribution is summed up. To compare the relative stability of CDplexes derived from the different CDs in this study in a biological medium, competitive displacement assays were performed using the polyanionic polysaccharide heparin[46,47] as displacing competitor and a fixed incubation time (10 min). The process was indirectly followed by monitoring the fluorescence intensity of a DNA intercalating agent.[31] CDplexes were formulated at N/P 5, thus ensuring complete DNA protection and a weak residual fluorescence background. Incubation of the CDplexes in the presence of increasing concentrations of heparin displayed very dissimilar profiles (Fig. 5). CDplexes formulated with 7_{But} and 7_{Hex} were rather invulnerable to heparin-induced disassembling up to the maximum concentration tested (2 mg mL^{-1}). The stability slightly decreased for CDplexes formulated with 7_{Pr} and was very limited for 7_{Ac}, for which the maximum fluorescence intensity, meaning total DNA release, is recovered with less than 50 μg mL^{-1} of heparin. The observed CDplex stability trend is inversed as compared with the tendency of the paCD to form 10–20 nm nanoaggregates as inferred from the TEM analysis. The results support the hypothesis that the capacity of facial amphiphiles to complex and release DNA is closely related to the balance between their tendency to form single-component self-assembled constructs *versus* their propensity to undergo DNA-

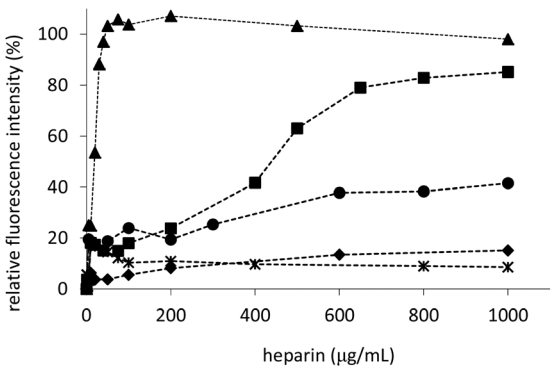

Fig. 5 Concentration-dependent heparin-induced CDplex dissociation: RedSafe™ fluorescence recovery upon incubation of CDplexes formulated at N/P 5 with ctDNA and 7-cationic centre CDs 7_H (■), 7_{Ac} (▲), 7_{Pr} (●), 7_{But} (◆), and 7_{Hex} (✳) with different amounts of heparin for 10 min. The fluorescence increase is due to the intercalation of the probe into ctDNA released from dissociated CDplexes.

templated alignment into multilayered architectures, which can be finely tuned by adjusting the HLB.

It is interesting to note that CDplexes formulated with the non-amphiphilic CD $\mathbf{7_H}$ resisted better than the acetylated analogue $\mathbf{7_{Ac}}$ against heparin-promoted dissociation; maximum fluorescence could only be recovered at concentrations >1 mg mL^{-1}. In this case the mechanism depicted in Fig. 1 is not operative and a different supramolecular organization must take place. Results obtained with the **21**-cationic centre paCD series were qualitatively similar.

CDplex dissociation dynamics. The above competition assay provides a "steady-state" vision of CDplex stability and propensity to release the DNA cargo. Yet, assessing the dynamics of the disassembly process is additionally necessary to properly interpret the effect of structural features of the vector in DNA delivery capabilities. Towards this end, CDplex stability was next probed in a similar experimental setup over time at a fixed heparin ratio (0.8 mg mL^{-1}). As illustrated in Fig. 6 for the CDplexes formulated with CDs of the **21**-series, dissociation kinetics are drastically influenced by acyl chain length, paralleling concentration-dependent experiments: fluorescence recovery, therefore DNA release, is much faster for CDs endowed with the shorter acetyl or propyl chains as compared with the butanoylated or hexanoylated derivatives (Fig. 6).

For comparative purposes, the same experiment was run on polyplexes formulated with bPEI (25 kDa) at the optimal transfection conditions (*i.e.* N/P 10). The experiment indicated a dissociation rate intermediate between that of $\mathbf{21_{Pr}}$ and $\mathbf{21_{But}}$ or $\mathbf{21_{Hex}}$ CDplexes (Fig. S35†). The non-amphiphilic derivative $\mathbf{21_H}$ (blue line, Fig. 6) again challenged the tendency of its amphiphilic counterparts. The dissociation of these CDplexes seems to be retarded at the beginning and slowly begins after *ca*. 200 min, which resembles the tendency displayed by bPEI polyplexes (see Fig. S35†) and might be illustrative of the purely electrostatic interactions involved in these systems. Nevertheless, stability of $\mathbf{21_H}$ CDplexes is far lower than that of bPEI polyplexes. The qualitative reliability of the experimental setup was confirmed at larger and shorter heparin concentrations that afforded the expected fluorescence recovery rate increase and decrease, respectively (data not shown).

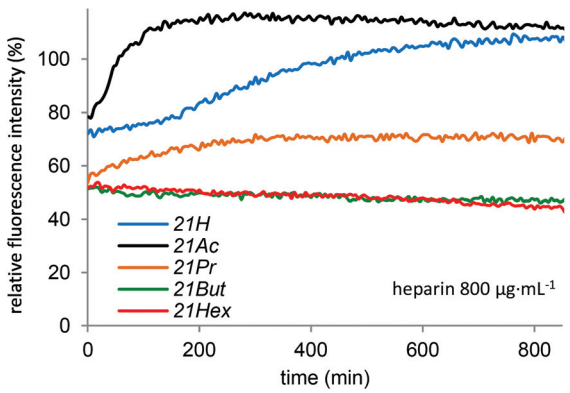

Fig. 6 Time-dependent heparin-induced CDplex dissociation. RedSafe™ fluorescence recovery upon incubation of CDplexes formulated at N/P 5 with ctDNA and **21**-cationic CDs $\mathbf{21_H}$ (blue), $\mathbf{21_{Ac}}$ (black), $\mathbf{21_{Pr}}$ (orange), $\mathbf{21_{But}}$ (green), and $\mathbf{21_{Hex}}$ (red) with heparin (800 µg mL^{-1}). Fluorescence increase is due to the intercalation of the probe into ctDNA released from dissociated CDplexes. Relative fluorescence levels correspond to solutions of the fluorescent probe in the absence (0%) and in the presence of ctDNA (100%). Note that initial measurement does not correspond necessarily with t = 0 minutes, since a few minutes (*ca*. 10 min) are required to set up the whole experiment.

Cell transfection capabilities of CDplexes

Gene carrier capabilities were assessed on African green monkey fibroblast-like COS-7 cells using a luciferase-encoding gene (pTG11236, pCMV-SV40-luciferase-SV40pA). Naked pDNA and JetPEI polyplexes were used as negative and positive controls, respectively. The assays were run with CDplexes formulated at N/P 2, 5 and 10 in 10% serum-containing medium. The level of exogenous luciferase expression (relative to the total amount of proteins) and the cell viability (relative to untreated controls) were measured for each CDplex formulation (Fig. 7; data at N/P 10 omitted for clarity; the full data set is collected in ESI, Fig. S36†).

The non-amphiphilic CDs $\mathbf{7_H}$ and $\mathbf{21_H}$ featured negligible gene transfer abilities under these experimental conditions,

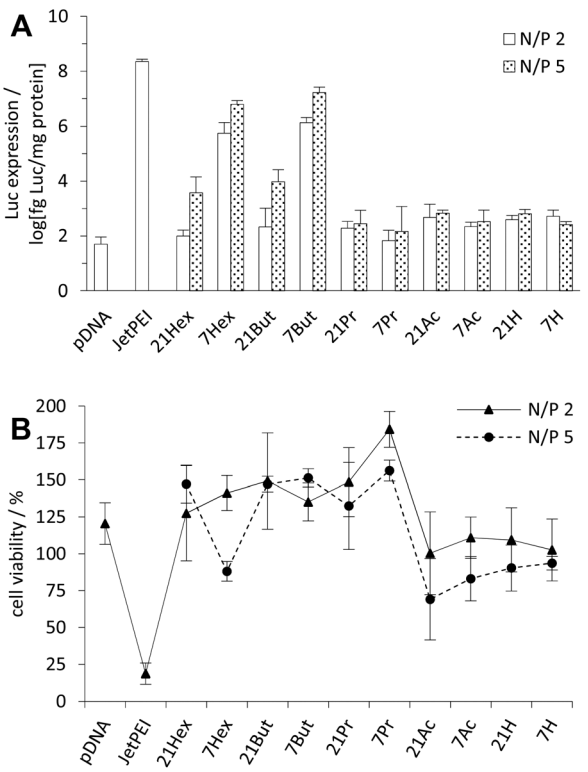

Fig. 7 *In vitro* transfection efficiency (panel A) and cell viability (panel B) in COS-7 cells in 10% serum-containing medium of CDplexes formulated with the luciferase encoding plasmid pTG11236 at N/P 2 (empty bars and triangles) and 5 (filled bars and circles). Naked pDNA and JetPEI polyplexes (N/P 10) were used as negative and positive controls, respectively. Experiments were run by triplicate.

regardless the N/P ratio (Fig. 7A), which might be explained on the basis of their modest DNA compacting capabilities in the light of the above experimental evidence. Only a modest luciferase expression increase is noticed at N/P 10 for the heptacationic $\mathbf{7_H}$ derivative, but with an intolerable toxicity (Fig. S36†). Virtually the same results were observed for CDplexes formulated with the paCDs featuring the shorter acyl chains (acetyl and propanoyls), regardless of the cationic density or N/P ratio. Similarly to their non-amphiphilic counterparts, toxicity is not an issue at low N/P ratios (2 and 5) but seriously increases at N/P 10, especially for the heptacationic derivatives (Fig. S36†). The inefficiency of these CDplexes to fulfil their task correlates with their relatively low stability, which probably leads to premature pDNA release.

CDplexes formulated with butanoylated and hexanoylated paCDs gradually increased their transfection efficiency with N/P ratio. At identical N/P ratio, the efficiency of derivatives with 7 cationic centres largely exceeded that of their 21-cationic analogues. Nevertheless, it must be recalled that N/P normalization implies a 3-fold higher molar proportion for the former. At N/P 5, paCDs $\mathbf{7_{But}}$ and $\mathbf{7_{Hex}}$ were revealed as the best carriers, only 10- and 30-fold less efficient than the gold standard JetPEI at its optimal N/P 10 ratio (Fig. 7A), and with a far milder cytotoxic profile (Fig. 7B). Indeed, efficiency could be further enhanced at N/P 10 for $\mathbf{7_{But}}$ up to parallel JetPEI performance, but at the cost of a significant drop in cell viability (Fig. S36†).

Fluorescence-assisted cell sorting (FACS) experiments using a fluorescently labelled plasmid (see ESI for experimental details, Fig. S37†) indicated that CDplex uptake is rather fast, since even the less stable CDplexes are detected inside COS-7 cells to a relevant extent after the incubation time (24 h). The question of whether further intracellular trafficking and fate is conditioned by inefficient endosomal release has been also addressed by performing transfection assays in the presence of the endosomolytic agent chloroquine. Luciferase expression promoted by $\mathbf{7_{But}}$ and $\mathbf{7_{Hex}}$ at N/P 5 was not affected in the presence of chloroquine and only a modest increase was detected for $\mathbf{21_{But}}$ and $\mathbf{21_{Hex}}$, indicating that endosome escape is not a bottleneck for transfection in these cases (Fig. S38†). The efficiency of the rest of formulations (already very poor) featured negligible variations. It can be speculated that efficient transfection requires the CDplexes to be sufficiently stable to remain assembled, providing full protection to the DNA cargo, in the early endosome at the vicinity of the cell membrane and undergo escape and DNA release upon acidification in the late endosome, near the nucleus, before lysosome fusion. Indeed, pDNA diffusion in the cytoplasm will be too slow to allow the nucleus to be reached before digestion by cytoplasmic nucleases.[48] CDplexes formulated with paCDs equipped with butanoyl and hexanoyl chains are not only more stable than CDplexes formulated with shorter-acyl-chain paCDs, but also exhibited significantly larger pH buffering capabilities (Table S1 and Fig. S32, S33†), probably benefitting from a proton sponge-type behaviour similar to that postulated for PEI-based carriers,[49] which prevents premature disassembly.

Conclusions

Correlation of non-viral gene carrier topology with transfection efficiency is often impaired by the limited control over the vector structure due to polydispersity or the lack of diversity-oriented synthetic tools. The body of work here discussed provides a proof of concept of the potential of strategies based on monodisperse molecular entities and flexible synthetic strategies, for structure–activity relationship analysis, tailoring of the self-assembly properties of CD-based vectors and optimization of gene delivery efficiencies. Variations in nucleic acid compaction, nanocomplex stability and transfection capabilities within series of homologous βCD-based facial amphiphiles have been correlated with their HLB. The library member incorporating a cationic corona with seven 2-aminoethylthioureido moieties on the primary rim and a multitail lipophilic domain of 14 butanoyl chains at the secondary rim, namely $\mathbf{7_{But}}$, was found to feature the best suited properties. The HLB in $\mathbf{7_{But}}$ seems to be optimal to both electrostatically interact with polyphosphate backbones and promote desolvation and compaction of DNA through hydrophobic interactions, leading to the spontaneous formation of nanoparticles where the gene material is fully protected from the environment. As described in previous studies on related structures,[50] these nanocomplexes might be stable enough to remain assembled in the early endosome after cellular uptake, enabling active trafficking in the cytoplasm and release of the DNA cargo at the nucleus vicinity. The flexibility of the strategy and its potential to pinpoint minute aspects of the relationship between macromolecular structure and functional capabilities offer new perspectives in the field.

Experimental

General methods

Reagents and solvents were purchased from commercial sources and used without further purification. NMR spectra were recorded at 500 MHz. 2D COSY, HSQC, and 1D TOCSY experiments were used to assist NMR assignments. Electrospray mass spectra (ESIMS) were obtained with a Bruker Esquire6000 instrument. Compounds **1**, **2**, **5**, **6**, **10**, **11**, **14**, **15**, **18**, $\mathbf{7_H}$, $\mathbf{7_{Hex}}$, $\mathbf{21_H}$, and $\mathbf{21_{Hex}}$ were synthesized as previously reported.[33,44]

Preparation of CD : DNA CDplexes

Two different nucleic acids were used: DNA sodium salt from calf thymus (ctDNA) and the luciferase-encoding plasmid pTG11236 (pCMVSV40-luciferase-SV40pA),[51] a 5739 bp plasmid. Due to the scarce pDNA sample availability, ctDNA was used for most physicochemical characterization studies, while pDNA was utilized in transfection assays. Eventually, comparative CDplex formation tests in the presence of both, ctDNA and pDNA, were carried out to validate ctDNA as pDNA surrogate. The quantities of compound used were calculated according to the desired DNA concentration, the N/P ratio, the

molecular weight and the number of protonatable nitrogen atoms in the corresponding cationic CD. JetPEI and bPEI (25 kDa) were used as standard references. In particular, DNA concentrations applied were 60 μg mL^{-1} (*i.e.* 180 μM phosphate) for gel electrophoresis, 20 μg mL^{-1} (*i.e.* 60 μM phosphate) for nanoparticle size, polydispersity index (PDI) and ζ potential measurements, 100 μg mL^{-1} (*i.e.* 303 μM phosphate) for transmission electron microscopy, 2 μg mL^{-1} (*i.e.* 6 μM phosphate) for fluorimetric DNA : paCD binding studies, 4 μg mL^{-1} (*i.e.* 12 μM phosphate) for heparin competitive displacement assays and 5 μg mL^{-1} (*i.e.* 15 μM phosphate) for *in vitro* transfection experiments.

For the preparation of CDplexes, typically DNA was diluted in HEPES (20 mM, pH 7.4) to the desired final concentration as specified above, and then the desired amount of CD derivative was dispersed in this solution from a stock solution in DMSO (typically 1–10 mM). The resulting mixture (with a final DMSO content below 1% in all cases) was instantly vortexed thoroughly and the complexes were incubated for one hour prior to subjecting them to characterization or transfection experiments.

CDplex characterization

Particle size, polydispersity index (PDI) and ζ potential were determined by dynamic light scattering (DLS) using a Zetasizer Nano (Malvern) with the following settings: automatic sampling time; three measurements per sample; medium viscosity, 1.054 cP; refractive index, 1.33; scattering angle, 173°; λ 633 nm; medium dielectric constant, 80; temperature, 25 °C; beam mode F(Ka) 1.5 (Smoluchowsky). Data were analyzed making use of the multimodal number distribution software included in the instrument. Results are presented as volume distribution of the major population by the mean diameter and its standard deviation. Before each series of experiments, the performance of the instrument was calibrated with either 90 nm monodisperse latex beads for DLS or with DTS 50 standard solution for ζ potentials. Experiments were run in triplicate.

Agarose gel electrophoresis shift assays were run in 0.8% (w/w) agarose gel in TAE buffer (1 : 1 : 1 Tris/acetate/EDTA) and stained with GelRed™ (Biotium). CDplexes were prepared as above described according to the desired ctDNA concentration (180 μM phosphate) at N/P ratios ranging from 0.5 to 20. The samples were prepared by mixing 18 μL of each CDplex formulation and 2 μL of loading buffer (5 mL glycerol, 250 μL TAE, 1 mL bromophenol blue and 2.75 mL water). The samples were submitted to electrophoresis for approximately 20 min at 150 V. DNA was visualized after photographing (λ 302 nm) using a transilluminator.

Transmission electron microscopy

Formvar-carbon-coated grids previously made hydrophilic by glow discharge were placed on top of small drops of the CDplex samples (HEPES 20 mM, pH 7.4, pDNA 303 μM phosphate) prepared as described above. After 1–3 min of contact, grids were negatively stained with a few drops of 1% aqueous solution of uranyl acetate. The grids were then dried and observed using a Philips CM12 electron microscope working under standard conditions. All these experiments were reproduced twice on each formulation.

CDplex formation and dissociation dynamics

CDplex formation and dissociation was monitored by fluorescence quenching of an intercalating agent. Experiments were performed on a Varian Cary Eclipse Fluorescence Spectrophotometer using ctDNA (2 μg mL^{-1}, 6 μM phosphate). For CDplex formation studies, a solution of staining agent RedSafe™ (iNtRON Biotechnology) was prepared. RedSafe™ fluorescence emission was measured at 525 nm (λ_{ex} 295 nm). Fluorescence emission of the buffer solution was taken as reference. When ctDNA was added to the RedSafe™ buffer solution (final concentration 3 μM phosphate), the fluorescence reading of the RedSafe™-DNA solution increased drastically. To this solution, aliquots of stock solutions of the corresponding paCD derivative in DMSO (50–1000 μM) μL portions were added in order to obtain ascending N/P ratios from 0.1 to 10 approximately. These N/P ratios correspond to CD concentrations ranging from *ca.* 0.03 to 8.6 μM. Fluorescence emission was recorded after each addition following equilibration (5 min). As the N/P ratio increases, fluorescence intensity decreases, indicating that DNA condensation and subsequent dye exclusion by CDplex formation is taking place. Aliquots of the paCD stock solution were added until no further decrease in fluorescence intensity could be observed.

To assess the relative stability of CDplexes, competitive displacement assays were performed on CDplexes at N/P ratio 5 using heparin. The effect of heparin on the CDplexes dissociation was evaluated by means of the change in relative fluorescence intensity obtained with the fluorescence probe RedSafe™. CDplexes were formulated from a 6 μM (phosphate) ctDNA solution in HEPES (20 mM, pH 7.4) containing RedSafe™. Aliquots of 150 μL of these CDplexes were transferred to the wells of a 96-well plate. Then, different volumes of heparin from stock solutions (100–10 000 μg mL^{-1} in HEPES 20 mM, pH 7.4) were added to each well and the final volume was adjusted to 250 μL (final heparin concentrations in the range of 5–2000 μg mL^{-1}). The plates were incubated for 10 min at rt prior to time-dependent fluorescence intensity measurements with a Varian Cary Eclipse Fluorescence Spectrophotometer equipped with a microplate reader, as indicated above. Naked ctDNA and bPEI were processed in a similar manner as indicated for the CDplexes and used as references.

In vitro transfection

Twenty-four hours before transfection, COS-7 cells were grown at a density of 2×10^4 cells per well in 96-well plates in Dulbecco modified Eagle culture medium (DMEM; Gibco-BRL) containing 10% foetal calf serum (FCS; Sigma) in a wet (37 °C) and 5% CO_2/95% air atmosphere. The paCD /pDNA CDplexes or bPEI/pDNA polyplexes were diluted to 100 μL in DMEM in order to have 0.5 μg of DNA in the preparation. The culture

medium was removed and replaced by 100 μL of the complexes in DMEM. After 4 h and 24 h, 50 and 100 μL of DMEM supplemented with 30% and 10% FCS, respectively, were added. After 48 h, the transfection was stopped, the culture medium was discarded, and the cells washed twice with 100 μL of PBS and lysed with 50 μL of lysis buffer (Promega). The lysates were frozen at −32 °C, before the analysis of luciferase activity. This measurement was performed in a LB96P luminometer (Berthold) in dynamic mode, for 10 s on 10 mL on the lysis mixture and using the "luciferase" determination system (Promega) in 96-well plates. The total protein concentration per well was determined by the BCA test (Thermo Scientific™ Pierce™ BCA protein assay kit), according to the supplier specifications. Luciferase activity was calculated as femtograms (fg) of luciferase per mg of protein. The percentage of cell viability of the nanocomplexes was calculated as the ratio of the total protein amount per well of the transfected cells relative to that measured for untreated cells × 100%.

In vitro transfection in the presence of endosomolytic agent

After twenty-four hours of cell culture, the complex CD derivative/DNA or PEI/DNA were diluted to 100 μL in DMEM containing 100 μM chloroquine (Sigma-Aldrich). The culture medium was removed from the cells and replaced by the solution of complexes. After 4 h of transfection in the presence of endosomolytic agent, the culture medium was aspirated, and the cells washed with 100 μL of PBS and covered by 150 μL of DMEM supplemented with 10% FCS. Another 100 μL of 10% FCS DMEM were added after 24 h of transfection. After 48 h, the transfection was stopped and the protocol was continued as described above.

Synthesis

Heptakis[6-(2-*tert*-butoxycarbonylaminoethylthio)-2,3-di-*O*-propanoyl]-cyclomaltoheptaose (3). To a solution of **1** [33] (1.0 g, 0.44 mmol) in dry DMF (30 mL) under nitrogen atmosphere, DMAP (2.28 g, 18.7 mmol, 3 eq.) and propanoic anhydride (3.2 mL, 24.9 mmol, 4 eq.) were added at 0 °C. The reaction mixture was allowed to warm to rt and stirred overnight. Then, MeOH (130 mL) was added and the reaction mixture was further stirred for 1 h. The solvents were removed under reduced pressure and H_2O (60 mL) was added to the reaction mixture, which was then extracted with DCM (4 × 60 mL). The organic layer was successively washed with 1 N aq. HCl (2 × 50 mL) and a saturated aqueous solution of $NaHCO_3$ (50 mL), dried over Na_2SO_4, filtered and reduced in vacuum. The crude product was purified by flash column chromatography (1 : 2 → 1 : 1 EtOAc–petroleum ether) to yield **3** (0.98 g, 73%). R_f = 0.29 (20 : 1 DCM–MeOH). $[\alpha]_D$ = +85.7 (c = 1.0 in DCM). ^{1}H NMR (500 MHz, $CDCl_3$): δ = 5.45 (bs, 7 H, N*H*Boc), 5.28 (t, 7 H, $J_{2,3}$ = $J_{3,4}$ = 8.9 Hz, H-3), 5.12 (d, 7 H, $J_{1,2}$ = 3.9 Hz, H-1), 4.84 (dd, 7 H, H-2), 4.20 (m, 7 H, H-5), 3.80 (t, 7 H, $J_{4,5}$ = 8.6 Hz, H-4), 3.35 (bq, 14 H, $^3J_{H,H}$ = 6.5 Hz, CH_2NHBoc), 3.17 (dd, 7 H, $J_{5,6a}$ = 2.1 Hz, $J_{6a,6b}$ = 11.7 Hz, H-6a), 3.07 (dd, 7 H, $J_{5,6b}$ = 5.9 Hz, H-6b), 2.79, 2.77 (2 dt, 14 H, $^2J_{H,H}$ = 13.4 Hz, $^3J_{H,H}$ = 6.7 Hz, CH_2S$_{Cyst}$), 2.47–2.20 (m, 28 H, CH_2CO), 1.47 (s, 63 H, CMe$_3$), 1.12 (2 t, 42 H, $^3J_{H,H}$ = 7.5 Hz, CH_3); ^{13}C NMR (125.7 MHz, $CDCl_3$): δ = 174.1, 172.6 (2 CO ester), 156.0 (CO carbamate), 96.8 (C-1), 79.4 (*C*Me$_3$), 79.0 (C-4), 71.3 (C-5), 70.7 (C-3), 70.2 (C-2), 40.4 (*C*H$_2$NHBoc), 33.8 (CH$_2$S$_{Cyst}$, C-6), 28.5 (C*Me*$_3$), 27.3, 27.2 (*C*H$_2$CO), 8.9 (CH_3). ESI-MS: m/z 1540.3 $[M + 2\ Na]^{2+}$, 3057.0 $[M + Na]^+$. Elemental analysis calculated (%) for $C_{133}H_{217}N_7O_{56}S_7$: C 52.64, H 7.21, N 3.23, S 7.40; found: C 52.64, H 7.27, N 3.20, S 7.69.

Heptakis[2,3-di-*O*-butanoyl-6-(2-*tert*-butoxycarbonylaminoethylthio)]cyclomaltoheptaose (4). To a solution of **1** [33] (1.21 g, 0.54 mmol) in dry DMF (40 mL) under nitrogen atmosphere, DMAP (2.77 g, 22.7 mmol, 3 eq.) and butanoic anhydride (4.9 mL, 30.2 mmol, 4 eq.) were added at 0 °C. The reaction mixture was allowed to warm to rt and stirred overnight. Then, MeOH (150 mL) was added and the reaction mixture was further stirred for 1 h. The solvents were removed under reduced pressure and H_2O (70 mL) was added to the reaction mixture, which was then extracted with DCM (4 × 70 mL). The organic layer was successively washed with 1 N aq. HCl (2 × 60 mL) and a saturated aqueous solution of $NaHCO_3$ (60 mL), dried over Na_2SO_4, filtered and reduced under vacuum. The crude product was purified by flash column chromatography (1 : 3 → 1 : 1 EtOAc–petroleum ether) to yield **4** as a white powder (1.36 g, 78%). R_f = 0.31 (20 : 1 DCM–MeOH). $[\alpha]_D$ = +101.6 (c = 1.0 in DCM). ^{1}H NMR (500 MHz, $CDCl_3$): δ = 5.47 (bs, 7 H, N*H*Boc), 5.29 (t, 7 H, $J_{2,3}$ = $J_{3,4}$ = 8.8 Hz, H-3), 5.14 (d, 7 H, $J_{1,2}$ = 3.9 Hz, H-1), 4.82 (dd, 7 H, H-2), 4.19 (m, 7 H, H-5), 3.81 (t, 7 H, $J_{4,5}$ = 8.6 Hz, H-4), 3.34 (bq, 14 H, $^3J_{H,H}$ = 6.5 Hz, CH_2NHBoc), 3.16 (dd, 7 H, $J_{5,6a}$ = 2.1 Hz, $J_{6a,6b}$ = 11.8 Hz, H-6a), 3.07 (dd, 7 H, $J_{5,6b}$ = 5.8 Hz, H-6b), 2.79, 2.77 (2 dt, 14 H, $^2J_{H,H}$ = 13.1 Hz, $^3J_{H,H}$ = 6.6 Hz, CH_2S$_{Cyst}$), 2.42–2.14 (m, 28 H, CH_2CO), 1.63 (m, 28 H, CH_2CH$_3$), 1.47 (s, 63 H, CMe$_3$), 0.98, 0.94 (2 t, 42 H, $^3J_{H,H}$ = 7.5 Hz, CH_3); ^{13}C NMR (125.7 MHz, $CDCl_3$): δ = 173.2, 171.6 (2 CO ester), 156.0 (CO carbamate), 96.5 (C-1), 79.3 (*C*Me$_3$), 78.8 (C-4), 71.3 (C-5), 70.4 (C-3), 70.1 (C-2), 40.4 (*C*H$_2$NHBoc), 35.9, 35.7 (*C*H$_2$CO), 33.8 (CH$_2$S$_{Cyst}$, C-6), 28.5 (C*Me*$_3$), 18.1 (*C*H$_2$CH$_3$), 13.6, 13.5 (CH_3). ESI-MS: m/z 1638.4 $[M + 2\ Na]^{2+}$, 3253.4 $[M + Na]^+$. Elemental analysis calculated (%) for $C_{147}H_{245}N_7O_{56}S_7$: C 54.65, H 7.64, N 3.03, S 6.95; found: C 54.81, H 7.34, N 2.87, S 6.97.

Heptakis[6-(2-aminoethylthio)-2,3-di-*O*-propanoyl]cyclomaltoheptaose (8). Treatment of heptacarbamate **3** (0.31 g, 0.10 mmol) with a 1 : 1 TFA–DCM mixture at rt for 2 h, followed by repeated co-evaporation with water and freeze-drying from a 0.1 N aq. HCl solution, gave pure compound **8** as its heptahydrochloride salt in quantitative yield (262 mg). $[\alpha]_D$ = +59.2 (c = 1.0 in MeOH). ^{1}H NMR (500 MHz, MeOD): δ = 5.42 (t, 7 H, $J_{2,3}$ = $J_{3,4}$ = 9.5 Hz, H-3), 5.26 (d, 7 H, $J_{1,2}$ = 3.6 Hz, H-1), 4.85 (dd, 7 H, H-2), 4.15 (m, 7 H, H-5), 3.99 (t, 7 H, $J_{4,5}$ = 9.0 Hz, H-4), 3.30 (t, 14 H, $^3J_{H,H}$ = 7.0 Hz, CH_2NH$_2$), 3.19–3.12 (m, 21 H, H-6a, CH_2S$_{Cyst}$), 3.07 (m, 7 H, H-6b), 2.51–2.30 (m, 28 H, CH_2CO), 1.15 (2 t, 42 H, $^3J_{H,H}$ = 7.5 Hz, CH_3); ^{13}C NMR (125.7 MHz, MeOD): δ = 173.9, (2 CO ester), 96.4 (C-1), 78.2 (C-4), 72.4 (C-5), 70.5 (C-3), 70.4 (C-2), 38.9 (*C*H$_2$NH$_2$), 33.2 (C-6), 30.3 (CH$_2$S$_{Cyst}$), 27.1, 26.9 (*C*H$_2$CO), 7.9 (CH_3). ESI-MS: m/z 1167.4 $[M + 2\ H]^{2+}$, 2333.9 $[M + H]^+$. Elemental analysis

calculated (%) for $C_{98}H_{168}Cl_7N_7O_{42}S_7{\cdot}7H_2O$: C 43.35, H 6.76, N 3.61, S 8.27; found: C 43.42, H 6.53, N 3.72, S 7.90.

Heptakis[6-(2-aminoethylthio)-2,3-di-*O*-butanoyl]cyclomaltoheptaose (9). Treatment of heptacarbamate **4** (0.30 g, 93 μmol) with TFA following the procedure described for the synthesis of compound **8**, followed by freeze-drying from a 0.1 N aq. HCl solution, gave pure compound **9** as its heptahydrochloride salt in quantitative yield (0.26 g). $[\alpha]_D$ = +65.0 (c = 1.0 in MeOH). ^{1}H NMR (500 MHz, MeOD, 313 K): δ = 5.40 (t, 7 H, $J_{2,3}$ = $J_{3,4}$ = 9.3 Hz, H-3), 5.22 (d, 7 H, $J_{1,2}$ = 3.5 Hz, H-1), 4.83 (dd, 7 H, H-2), 4.14 (m, 7 H, H-5), 3.94 (t, 7 H, $J_{4,5}$ = 8.7 Hz, H-4), 3.32–3.26 (m, 21 H, CH_2NH$_2$, H-6a), 3.13–2.98 (m, 21 H, H6-b, CH_2S$_{Cyst}$), 2.49–2.25 (m, 28 H, CH_2CO), 1.67 (m, 28 H, CH_2CH$_3$), 0.98, 0.99 (2 t, 42 H, $^3J_{H,H}$ = 7.4 Hz, CH$_3$); ^{13}C NMR (125.7 MHz, MeOD, 313 K): δ = 173.0, 172.8 (2 CO ester), 96.5 (C-1), 78.4 (C-4), 72.5 (C-5), 70.4 (C-3), 70.1 (C-2), 39.0 (*C*H$_2$NH$_2$), 35.7, 35.5 (*C*H$_2$CO), 33.3 (C-6), 30.4 (CH$_2$S$_{Cyst}$), 17.8 (*C*H$_2$CH$_3$), 12.6 (CH$_3$). ESI-MS: m/z 1265.6 [M + 2 H]$^{2+}$, 2530.1 [M + H]$^+$. Elemental analysis calculated (%) for $C_{112}H_{196}Cl_7N_7O_{42}S_7{\cdot}7H_2O$: C 46.20, H 7.27, N 3.37, S 7.71; found: C 45.89, H 6.91, N 3.19, S 7.63.

Heptakis[6-(2-(*N*′-(2-*tert*-butoxycarbonylaminoethyl)thioureido)ethylthio)-2,3-di-*O*-propanoyl]cyclomaltoheptaose (12). To a solution of compound **8** (100 mg, 39 μmol) and Et$_3$N (94 μL, 0.68 mmol, 2.5 eq.) in DCM (2 mL) a solution of 2-(*tert*-butoxycarbonylamino)ethyl isothiocyanate[43] (66 mg, 0.32 mmol, 1.2 eq.) in DCM (1 mL) was added dropwise. The reaction mixture was stirred overnight at rt. After evaporation of the solvent under reduced pressure, the residue was purified by flash column chromatography (40 : 1 → 15 : 1 DCM–MeOH) to yield compound **12** as an off-white powder (108 mg, 75%). R_f = 0.19 (20 : 1 DCM–MeOH). $[\alpha]_D$ = +73.9 (c = 1.0 in DCM). ^{1}H NMR (500 MHz, CDCl$_3$): δ = 7.25 (2 bs, 14 H, NHCS), 5.63 (bs, 7 H, N*H*Boc), 5.27 (t, 7 H, $J_{2,3}$ = $J_{3,4}$ = 8.5 Hz, H-3), 5.11 (d, 7 H, $J_{1,2}$ = 2.7 Hz, H-1), 4.82 (dd, 7 H, H-2), 4.20 (m, 7 H, H-5), 3.78 (t, 7 H, $J_{4,5}$ = 8.2 Hz, H-4), 3.73, 3.61 (2 m, 28 H, CH_2NHCS), 3.30 (bs, 14 H, CH_2NHBoc), 3.22 (bd, 7 H, $J_{6a,6b}$ = 13.1 Hz, H-6a), 3.04 (m, 7 H, H-6b), 2.95, 2.83 (2 m, 14 H, CH_2S$_{Cyst}$), 2.42–2.17 (m, 28 H, CH_2CO), 1.45 (s, 63 H, CMe$_3$), 1.12, 1.10 (2 t, 42 H, $^3J_{H,H}$ = 7.5 Hz, CH$_3$); ^{13}C NMR (125.7 MHz, CDCl$_3$, 313 K): δ = 182.3 (CS), 174.1, 173.1 (2 CO ester), 157.3 (CO carbamate), 96.7 (C-1), 79.0 (*C*Me$_3$), 78.3 (C-4), 71.8 (C-5), 70.8 (C-3), 70.4 (C-2), 43.8 (*C*H$_2$NHCS), 39.6 (*C*H$_2$NHBoc), 33.7 (C-6), 32.7 (CH$_2$S$_{Cyst}$), 27.6 (C*Me*$_3$), 27.1, 27.0 (*C*H$_2$CO), 8.0 (CH$_3$). ESI-MS: m/z 1286.3 [M + 2 Na + K]$^{3+}$, 1897.8 [M + 2 Na]$^{2+}$, 1917.5 [M + Na + K]$^{2+}$. Elemental analysis calculated (%) for $C_{154}H_{259}N_{21}O_{56}S_{14}$: C 49.33, H 6.96, N 7.84, S 11.97; found: C 49.25, H 7.17, N 7.55, S 11.93.

Heptakis[2,3-di-*O*-butanoyl-6-(2-(*N*′-(2-*tert*-butoxycarbonylaminoethyl)thioureido)ethylthio)]cyclomaltoheptaose (13). To a solution of compound **9** (81 mg, 29 μmol) and Et$_3$N (71 μL, 0.51 mmol, 2.5 eq.) in DCM (2 mL) a solution of 2-(*tert*-butoxycarbonylamino)ethyl isothiocyanate[43] (49 mg, 0.24 mmol, 1.2 eq.) in DCM (1 mL) was added dropwise. The reaction mixture was stirred overnight at rt. Then, the solvent was evaporated under reduced pressure and the resulting residue was purified by flash column chromatography (40 : 1 → 15 : 1 DCM–MeOH) to yield compound **13** as an off-white powder (97 mg, 84%). R_f = 0.20 (20 : 1 DCM–MeOH). $[\alpha]_D$ = +38.5 (c = 1.0 in DCM). ^{1}H NMR (500 MHz, MeOD, 313 K): δ = 5.36 (t, 7 H, $J_{2,3}$ = $J_{3,4}$ = 8.2 Hz, H-3), 5.19 (d, 7 H, $J_{1,2}$ = 2.7 Hz, H-1), 4.83 (dd, 7 H, H-2), 4.23 (m, 7 H, H-5), 3.96 (t, 7 H, $J_{4,5}$ = 8.0 Hz, H-4), 3.77, 3.60 (2 m, 28 H, CH_2NHCS), 3.28 (m, 21 H, CH_2NHBoc, H-6a), 3.20 (dd, 7 H, $J_{5,6a}$ = 4.1 Hz, $J_{6a,6b}$ = 9.8 Hz, H-6b), 2.97, 2.93 (2 m, 14 H, CH_2S$_{Cyst}$), 2.46–2.23 (m, 28 H, CH_2CO), 1.67 (m, 28 H, CH_2CH$_3$), 1.47 (s, 63 H, CMe$_3$), 1.00, 0.97 (2 t, 42 H, $^3J_{H,H}$ = 7.2 Hz, CH$_3$). ^{13}C NMR (125.7 MHz, 313 K, MeOD): δ = 182.2 (CS), 173.1, 172.0 (2 CO ester), 157.3 (CO carbamate), 96.5 (C-1), 79.0 (*C*Me$_3$), 78.2 (C-4), 71.9 (C-5), 70.5 (C-3), 70.3 (C-2), 43.9 (*C*H$_2$NHCS), 39.6 (*C*H$_2$NHBoc), 35.7, 35.6 (*C*H$_2$CO), 33.7 (C-6), 32.7 (CH$_2$S$_{Cyst}$), 27.6 (C*Me*$_3$), 17.9, 17.8 (*C*H$_2$CH$_3$), 12.7 (CH$_3$). ESI-MS: m/z 1995.6 [M + 2 Na]$^{2+}$, 3966.6 [M + Na]$^+$. Elemental analysis calculated (%) for $C_{168}H_{287}N_{21}O_{56}S_{14}$: C 51.13, H 7.33, N 7.45, S 11.38; found: C 51.34, H 7.36, N 7.48, S 11.29.

Heptakis[6-(2-(*N*′-(2-(*N*,*N*-di-(2-(*N*-*tert*-butoxycarbonylamino)ethyl)amino)ethyl)thioureido)ethylthio)-2,3-di-*O*-propanoyl]cyclomaltoheptaose (16). To a solution of compound **8** (95 mg, 37 μmol) and Et$_3$N (90 μL, 0.64 mmol, 2.5 eq.) in DCM (2 mL) a solution of 2-[bis(2-(*tert*-butoxycarbonylamino)ethyl)amino]ethyl isothiocyanate[33] (120 mg, 0.31 mmol, 1.2 eq.) in DCM (1 mL) was added dropwise. The reaction mixture was stirred overnight at rt. After evaporation of the solvent under reduced pressure, the residue was purified by flash column chromatography (40 : 1 → 15 : 1 DCM–MeOH) to yield compound **16** as an off-white powder (114 mg, 62%). R_f = 0.64 (9 : 1 DCM–MeOH). $[\alpha]_D$ = +37.8 (c = 1.0 in MeOH). ^{1}H NMR (500 MHz, MeOD, 323 K): δ = 5.36 (t, 7 H, $J_{2,3}$ = $J_{3,4}$ = 8.7 Hz, H-3), 5.18 (d, 7 H, $J_{1,2}$ = 3.3 Hz, H-1), 4.83 (dd, 7 H, H-2), 4.25 (m, 7 H, H-5), 3.97 (t, 7 H, $J_{4,5}$ = 8.3 Hz, H-4), 3.81 (bt, 14 H, CH_2CH$_2$S$_{Cyst}$), 3.56 (bt, 14 H, NCH$_2$CH_2NHCS), 3.23 (m, 42 H, H-6a, H-6b, CH_2NHBoc), 2.96 (m, 14 H, CH_2S$_{Cyst}$), 2.74 (t, 14 H, $^3J_{H,H}$ = 6.0 Hz, NCH_2CH$_2$NHCS), 2.64 (t, 28 H, $^3J_{H,H}$ = 6.0 Hz, CH_2CH$_2$NHBoc), 2.50–2.27 (m, 28 H, CH_2CO), 1.48 (s, 126 H, CMe$_3$), 1.15, 1.13 (2 t, 42 H, $^3J_{H,H}$ = 7.7 Hz, CH$_3$); ^{13}C NMR (125.7 MHz, MeOD, 313 K): δ = 182.3 (CS), 174.0, 173.1 (2 CO ester), 157.1 (CO carbamate), 96.7 (C-1), 78.9 (*C*Me$_3$), 78.4 (C-4), 71.8 (C-5), 70.8 (C-3), 70.4 (C-2), 54.3 (*C*H$_2$CH$_2$NHBoc), 53.3 (NCH_2CH$_2$NHCS), 44.0 (*C*H$_2$CH$_2$S$_{Cyst}$), 42.0 (NCH$_2$*C*H$_2$NHCS), 38.6 (*C*H$_2$NHBoc), 33.8 (C-6), 33.0 (CH$_2$S$_{Cyst}$), 27.7 (C*Me*$_3$), 27.1, 27.0 (*C*H$_2$CO), 8.1, 8.0 (CH$_3$). ESI-MS: m/z 1723.8 [M + 3 K]$^{3+}$, 2550.2 [M + 2 Na]$^{2+}$, 2558.3 [M + Na + K]$^{2+}$, 2543.4 [M + Cl − H]$^{2-}$. Elemental analysis calculated (%) for $C_{217}H_{385}N_{35}O_{70}S_{14}$: C 51.57, H 7.68, N 9.70, S 8.88; found: C 51.18, H 7.67, N 9.23, S 8.99.

Heptakis[2,3-di-*O*-butanoyl-6-(2-(*N*′-(2-(*N*,*N*-di-(2-(*N*-*tert*-butoxycarbonylamino)ethyl)amino)ethyl)thioureido)ethylthio)]cyclomaltoheptaose (17). To a solution of compound **9** (100 mg, 36 μmol) and Et$_3$N (87 μL, 0.63 mmol, 2.5 eq.) in DCM (2 mL) a solution of 2-[bis(2-(*tert*-butoxycarbonylamino)ethyl)amino]ethyl isothiocyanate[33] (117 mg, 0.30 mmol, 1.2 eq.) in DCM (1 mL) was added dropwise. The reaction mixture was stirred

overnight at rt. Then, the solvent was evaporated under reduced pressure and the resulting residue was purified by flash column chromatography (40 : 1 → 15 : 1 DCM–MeOH) to give compound **17** (139 mg, 74%). R_f = 0.63 (20 : 1 DCM–MeOH). $[\alpha]_D$ = +38.1 (*c* = 0.99 in MeOH). ^{1}H NMR (500 MHz, MeOD, 323 K): δ = 5.36 (t, 7 H, $J_{2,3} = J_{3,4}$ = 8.7 Hz, H-3), 5.17 (d, 7 H, $J_{1,2}$ = 3.7 Hz, H-1), 4.83 (dd, 7 H, H-2), 4.23 (m, 7 H, H-5), 3.97 (t, 7 H, $J_{4,5}$ = 8.3 Hz, H-4), 3.81 (t, 14 H, $^3J_{H,H}$ = 6.5 Hz, CH_2CH$_2$N$_{Cyst}$), 3.56 (m, 14 H, NCH$_2$CH_2NHCS), 3.29 (m, 7 H, H-6a), 3.21 (dd, 7 H, $J_{5,6b}$ = 5.0 Hz, $J_{6a,6b}$ = 14.3 Hz, H-6b), 3.16 (t, 28 H, $^3J_{H,H}$ = 6.5 Hz, CH_2NHBoc), 2.96 (m, 14 H, CH_2S$_{Cyst}$), 2.74 (t, 14 H, $^3J_{H,H}$ = 6.5 Hz, NCH_2CH$_2$NHCS), 2.53 (t, 28 H, $^3J_{H,H}$ = 6.5 Hz, CH_2CH$_2$NHBoc), 2.47–2.23 (m, 28 H, CH_2CO), 1.67 (m, 28 H, CH_2CH$_3$), 1.48 (s, 126 H, CMe$_3$), 1.01, 0.98 (2 t, 42 H, $^3J_{H,H}$ = 7.5 Hz, CH$_3$). ^{13}C NMR (125.7 MHz, MeOD, 313 K): δ = 173.1, 172.1 (2 CO ester), 157.1 (CO carbamate), 96.6 (C-1), 79.1 (*C*Me$_3$), 78.3 (C-4), 72.0 (C-5), 70.7 (C-3), 70.3 (C-2), 54.3 (*C*H$_2$CH$_2$NHBoc), 53.5 (N*C*H$_2$CH$_2$NHCS), 44.1 (*C*H$_2$CH$_2$S$_{Cyst}$), 41.9 (NCH$_2$*C*H$_2$NHCS), 38.4 (*C*H$_2$NHBoc), 35.8, 35.6 (*C*H$_2$CO), 34.0 (C-6), 33.0 (CH$_2$S$_{Cyst}$), 27.7 (C*Me*$_3$), 17.9, 17.8 (*C*H$_2$CH$_3$), 12.7 (CH$_3$). ESI-MS: *m*/*z* 1772.9 [M + 3 Na]$^{3+}$, 2647.9 [M + 2 Na]$^{2+}$. Elemental analysis calculated (%) for $C_{231}H_{413}N_{35}O_{70}S_{14}$: C 52.85, H 7.93, N 9.34, S 8.55; found: C 52.77, H 7.95, N 9.36, S 8.38.

Heptakis[2,3-di-*O*-acetyl-6-(2-(*N*′-(2-aminoethyl)thioureido)ethylthio)]cyclomaltoheptaose heptahydrochloride (7_{Ac}). Treatment of compound **11** [44] (50 mg, 14 μmol) with anhydrous TFA (100 μL) at rt for 5 min, followed by freeze-drying immediately from a 0.1 N aq. HCl solution, afforded pure paCD 7_{Ac} in virtually quantitative yield (43 mg). $[\alpha]_D$ = +35.2 (*c* = 0.5 in MeOH). ^{1}H NMR (500 MHz, DMSO-d_6, 333 K): δ = 8.12 (bs, 14 H, NH$_2$), 7.97, 7.75 (2 bs, 14 H, NHCS), 5.22 (t, 7 H, $J_{2,3} = J_{3,4}$ = 9.0 Hz, H-3), 5.11 (d, 7 H, $J_{1,2}$ = 3.7 Hz, H-1), 4.73 (dd, 7 H, H-2), 4.14 (m, 7 H, H-5), 3.90 (t, 7 H, $J_{4,5}$ = 8.8 Hz, H-4), 3.72, 3.63 (2 bq, 28 H, CH_2NHCS), 3.12 (m, 14 H, H-6a, H-6b), 3.02 (bt, 14 H, CH_2NH$_2$), 2.82 (m, 14 H, CH_2S$_{Cyst}$), 2.02, 2.00 (2s, 42 H, COCH$_3$); ^{13}C NMR (100.6 MHz, DMSO-d$_6$, 323 K): δ = 183.2 (CS), 170.5, 169.7 (2 CO ester), 97.0 (C-1), 78.8 (C-4), 71.6 (C-5), 70.8 (C-2, C-3), 44.0, 41.7 (*C*H$_2$NHCS), 38.8 (CH$_2$NH$_2$), 33.7 (C-6), 32.8 (CH$_2$S$_{Cyst}$), 21.0 (CO*C*H$_3$). ESI-MS: *m*/*z* 713.8 [M + 4 H]$^{4+}$, 951.7 [M + 3 H]$^{3+}$, 1426.7 [M + 2 H]$^{2+}$. Elemental analysis calculated (%) for $C_{105}H_{182}Cl_7N_{21}O_{42}S_{14}$: C 40.58, H 5.90, N 9.46, S 14.44; found: C 40.54, H 6.15, N 9.33, S 14.79.

Heptakis[6-(2-(*N*′-(2-aminoethyl)thioureido)ethylthio)-2,3-di-*O*-propanoyl]cyclomaltoheptaose heptahydrochloride (7_{Pr}). Treatment of heptacarbamate **12** (35 mg, 9.3 μmol) with anhydrous TFA (90 μL) at rt for 5 min, followed by freeze-drying immediately from a 0.1 N aq. HCl solution, yielded pure paCD 7_{Pr} (28 mg, 90%). $[\alpha]_D$ = +36.9 (*c* = 0.5 in MeOH). ^{1}H NMR (500 MHz, DMSO-d$_6$, 333 K): δ = 8.11 (bs, 14 H, NH$_2$), 7.96, 7.75 (2 bs, 14 H, NHCS), 5.24 (t, 7 H, $J_{2,3} = J_{3,4}$ = 8.9 Hz, H-3), 5.10 (d, 7 H, $J_{1,2}$ = 3.4 Hz, H-1), 4.74 (dd, 7 H, H-2), 4.16 (m, 7 H, H-5), 3.91 (t, 7 H, $J_{4,5}$ = 8.6 Hz, H-4), 3.71, 3.64 (2 bq, 28 H, CH_2NHCS), 3.12 (m, 14 H, H-6a, H-6b), 3.02 (bt, 14 H, CH_2NH$_2$), 2.83 (m, 14 H, CH_2S$_{Cyst}$), 2.37–2.20 (m, 28 H, CH_2CO), 1.04, 1.03 (2 t, 42 H, $^3J_{H,H}$ = 7.5 Hz, CH$_3$); ^{13}C NMR (125.7 MHz, DMSO-d$_6$, 323 K): δ = 183.2 (CS), 173.7, 172.9 (2 CO ester), 96.9 (C-1), 78.7 (C-4), 71.7 (C-5), 70.9 (C-3), 70.6 (C-2), 43.1, 41.7 (*C*H$_2$NHCS), 38.9 (*C*H$_2$NH$_2$), 33.8 (C-6), 32.8 (CH$_2$S$_{Cyst}$), 27.2 (*C*H$_2$CO), 9.1 (CH$_3$). ESI-MS: *m*/*z* 762.7 [M + 4 H]$^{4+}$, 1017.6 [M + 3 H]$^{3+}$, 1525.5 [M + 2 H]$^{2+}$, 3048.8 [M + H]$^+$. Elemental analysis calculated (%) for $C_{119}H_{210}Cl_7N_{21}O_{42}S_{14}$: C 43.26, H 6.41, N 8.90, S 13.59; found: C 43.34, H 6.33, N 8.84, S 13.34.

Heptakis[6-(2-(*N*′-(2-aminoethyl)thioureido)ethylthio)-2,3-di-*O*-butanoyl]cyclomaltoheptaose heptahydrochloride (7_{But}). Treatment of heptacarbamate **13** (88 mg, 22 μmol) with anhydrous TFA (0.5 mL) at rt for 5 min, followed by freeze-drying immediately from a 0.1 N aq. HCl solution, yielded pure paCD 7_{But} in quantitative yield (78 mg). $[\alpha]_D$ = +34.3 (*c* = 0.5 in MeOH). ^{1}H NMR (500 MHz, DMSO-d$_6$, 333 K): δ = 8.15 (bs, 14 H, NH$_2$), 7.97, 7.75 (2 bs, 14 H, NHCS), 5.26 (t, 7 H, $J_{2,3} = J_{3,4}$ = 8.8 Hz, H-3), 5.11 (d, 7 H, $J_{1,2}$ = 3.0 Hz, H-1), 4.73 (dd, 7 H, H-2), 4.17 (m, 7 H, H-5), 3.91 (t, 7 H, $J_{4,5}$ = 8.9 Hz, H-4), 3.73, 3.65 (2 bq, 28 H, CH_2NHCS), 3.11 (m, 14 H, H-6a, H-6b), 3.03 (bt, 14 H, CH_2NH$_2$), 2.84 (m, 14 H, CH_2S$_{Cyst}$), 2.34, 2.22 (2 m, 28 H, CH_2CO), 1.57 (m, 28 H, CH_2CH$_3$), 0.92, 0.89 (2 t, 42 H, $^3J_{H,H}$ = 7.4 Hz, CH$_3$); ^{13}C NMR (125.7 MHz, DMSO-d$_6$, 333 K): δ = 183.4 (CS), 172.8, 171.8 (2 CO ester), 96.7 (C-1), 78.6 (C-4), 71.6 (C-5), 70.7, 70.5 (C-3, C-2), 44.2, 43.1 (*C*H$_2$NHCS), 39.0 (*C*H$_2$NH$_2$), 35.8, 35.7 (*C*H$_2$CO), 34.1 (C-6), 32.9 (CH$_2$S$_{Cyst}$), 18.1, 18.0 (*C*H$_2$CH$_3$), 13.7 (CH$_3$). ESI-MS: *m*/*z* 812.5 [M + 4 H]$^{4+}$, 1082.4 [M + 3 H]$^{3+}$, 1623.1 [M + 2 H]$^{2+}$, 3245.1 [M + H]$^+$. Elemental analysis calculated (%) for $C_{133}H_{238}Cl_7N_{21}O_{42}S_{14}$: C 45.63, H 6.85, N 8.40, S 12.82; found: C 45.51, H 7.01, N 8.35, S 12.57.

Heptakis[2,3-di-*O*-acetyl-6-(2-(*N*′-(2-(*N*,*N*-di-(2-aminoethyl)amino)ethyl)thioureido)ethylthio)]cyclomaltoheptaose tetradecahydrochloride (21_{Ac}). Treatment of compound **15** (50 mg, 10 μmol) with anhydrous TFA (100 μL) at rt for 5 min, followed by freeze-drying immediately from a 0.1 N aq. HCl solution, afforded pure paCD 21_{Ac} in quantitative yield (41 mg). $[\alpha]_D$ = +25.1 (*c* = 0.5 in MeOH). ^{1}H NMR (500 MHz, 10 : 1 MeOD-D_2O, 333 K): δ = 5.33 (t, 7 H, $J_{2,3} = J_{3,4}$ = 8.8 Hz, H-3), 5.21 (d, 7 H, $J_{1,2}$ = 3.6 Hz, H-1), 4.83 (dd, 7 H, H-2), 4.20 (m, 7 H, H-5), 3.96 (t, 7 H, $J_{4,5}$ = 8.6 Hz, H-4), 3.88 (bt, 14 H, CH_2CH$_2$S$_{Cyst}$), 3.78 (bt, 14 H, NCH$_2$CH_2NHCS), 3.39 (m, 28 H, CH_2NH$_2$), 3.33–3.18 (m, 56 H, H-6a, H-6b, CH_2CH$_2$NH$_2$, NCH_2CH$_2$NHCS), 2.95 (m, 14 H, CH_2S$_{Cyst}$), 2.10, 2.08 (2s, 42 H, COCH$_3$); ^{13}C NMR (100.6 MHz, 15 : 1 MeOD-D_2O, 323 K): δ = 182.9 (CS), 171.3, 170.6 (2 CO ester), 96.7 (C-1), 78.7 (C-4), 72.1 (C-5), 70.9 (C-3, C-2), 52.7 (N*C*H$_2$CH$_2$NHCS), 51.1 (*C*H$_2$CH$_2$NH$_2$), 44.1 (*C*H$_2$CH$_2$S$_{Cyst}$), 40.4 (NCH$_2$*C*H$_2$NHCS), 36.4 (*C*H$_2$NH$_2$), 33.7 (C-6), 32.7 (CH$_2$S$_{Cyst}$), 19.9, 19.8 (CO*C*H$_3$). ESI-MS: *m*/*z* 691.7 [M + 5 H]$^{5+}$, 864.6 [M + 4 H]$^{4+}$, 1152.7 [M + 3 H]$^{3+}$, 1728.7 [M + 2 H]$^{2+}$. Elemental analysis calculated (%) for $C_{133}H_{259}Cl_{14}N_{35}O_{42}S_{14}$: C 40.28, H 6.58, N 12.36, S 11.32; found: C 40.10, H 6.66, N 12.56, S 11.32.

Heptakis[6-(2-(*N*′-(2-(*N*,*N*-di-(2-aminoethyl)amino)ethyl)thioureido)ethylthio)-2,3-di-*O*-propanoyl]cyclomaltoheptaose tetradecahydrochloride (21_{Pr}). Treatment of compound **16** (100 mg,

19.8 μmol) with anhydrous TFA (0.5 mL) at rt for 5 min, followed by freeze-drying immediately from a 0.1 N aq. HCl solution, afforded pure paCD **21$_{Pr}$** in quantitative yield (82 mg). $[\alpha]_D$ = +33.2 (*c* = 0.25 in MeOH). ^{1}H NMR (500 MHz, 10 : 1 MeOD–D_2O, 323 K): δ = 5.32 (t, 7 H, $J_{2,3} = J_{3,4}$ = 8.6 Hz, H-3), 5.18 (d, 7 H, $J_{1,2}$ = 3.5 Hz, H-1), 4.84 (dd, 7 H, H-2), 4.21 (m, 7 H, H-5), 3.96 (t, 7 H, $J_{4,5}$ = 8.3 Hz, H-4), 3.77 (bt, 14 H, CH_2CH$_2$S$_{Cyst}$), 3.72 (bt, 14 H, NCH$_2$CH_2NHCS), 3.23 (m, 42 H, H-6a, H-6b, CH_2NH$_2$), 3.00 (t, 28 H, $^3J_{H,H}$ = 5.9 Hz, CH_2CH$_2$NH$_2$), 2.94 (m, 14 H, CH_2S$_{Cyst}$), 2.89 (t, 14 H, $^3J_{H,H}$ = 5.9 Hz, NCH_2CH$_2$NHCS), 2.49–2.27 (m, 28 H, CH_2CO), 1.13, 1.11 (2 t, 42 H, $^3J_{H,H}$ = 7.5 Hz, CH$_3$); ^{13}C NMR (125.7 MHz, 5 : 1 MeOD–D_2O, 323 K): δ = 182.2 (CS), 174.9, 173.7 (2 CO ester), 96.6 (C-1), 78.3 (C-4), 72.0 (C-5), 70.9 (C-3), 70.4 (C-2), 52.2 (N*C*H$_2$CH$_2$NHCS), 51.0 (*C*H$_2$CH$_2$NH$_2$), 44.1 (*C*H$_2$CH$_2$S$_{Cyst}$), 40.8 (NCH$_2$*C*H$_2$NHCS), 36.8 (*C*H$_2$NH$_2$), 33.9 (C-6), 32.7 (CH$_2$S$_{Cyst}$), 27.2 (*C*H$_2$CO), 8.2, 8.1 (CH$_3$). ESI-MS: *m*/*z* 931.1 [M + H + 3 Na]$^{4+}$, 1239.9 [M + 3 Na]$^{3+}$, 1827.3 [M + 2 H]$^{2+}$. Elemental analysis calculated (%) for $C_{147}H_{287}Cl_{14}N_{35}O_{42}S_{14}\cdot 7H_2O$: C 41.17, H 7.07, N 11.43, S 10.47; found: C 40.93, H 6.89, N 11.35, S 10.22.

Heptakis[6-(2-(*N*′-(2-(*N*,*N*-di-(2-aminoethyl)amino)ethyl)thioureido)ethylthio)-2,3-di-*O*-butanoyl]cyclomaltoheptaose tetradecahydrochloride (21$_{But}$). Treatment of compound **17** (63 mg, 12 μmol) with anhydrous TFA (200 μL) at rt for 5 min, followed by freeze-drying immediately from a 0.1 N aq. HCl solution, afforded pure paCD **21$_{But}$** in virtually quantitative yield (51 mg). $[\alpha]_D$ = +30.0 (*c* = 0.5 in MeOH). ^{1}H NMR (500 MHz, 10 : 1 MeOD–D_2O, 333 K): δ = 5.33 (t, 7 H, $J_{2,3} = J_{3,4}$ = 8.6 Hz, H-3), 5.20 (d, 7 H, $J_{1,2}$ = 3.6 Hz, H-1), 4.86 (dd, 7 H, H-2), 4.20 (m, 7 H, H-5), 3.97 (t, 7 H, $J_{4,5}$ = 8.4 Hz, H-4), 3.84 (bt, 14 H, CH_2CH$_2$S$_{Cyst}$), 3.80 (bq, 14 H, NCH$_2$CH_2NHCS), 3.35 (t, 28 H, $^3J_{H,H}$ = 6.2 Hz, CH_2NH$_2$), 3.29 (m, 14 H, H-6a, H-6b), 3.24 (t, 28 H, $^3J_{H,H}$ = 7.4 Hz, CH_2CH$_2$NH$_2$), 3.11 (t, 14 H, $^3J_{H,H}$ = 6.4 Hz, NCH_2CH$_2$NHCS), 2.96 (m, 14 H, CH_2S$_{Cyst}$), 2.46–2.24 (m, 28 H, CH_2CO), 1.66 (m, 28 H, CH_2CH$_3$), 1.00, 0.96 (2 t, 42 H, $^3J_{H,H}$ = 7.5 Hz, CH$_3$); ^{13}C NMR (100.6 MHz, 10 : 1 MeOD–D_2O, 323 K): δ = 173.6, 172.3 (2 CO ester), 96.5 (C-1), 78.2 (C-4), 72.0 (C-5), 70.6 (C-3), 70.3 (C-2), 52.4 (N*C*H$_2$CH$_2$NHCS), 51.2 (*C*H$_2$CH$_2$NH$_2$), 44.1 (*C*H$_2$CH$_2$S$_{Cyst}$), 40.9 (NCH$_2$*C*H$_2$NHCS), 36.9 (*C*H$_2$NH$_2$), 35.7, 35.6 (*C*H$_2$CO), 33.9 (C-6), 32.7 (CH$_2$S$_{Cyst}$), 18.0, 17.9 (*C*H$_2$CH$_3$), 12.7 (CH$_3$). ESI-MS: *m*/*z* 978.3 [M + H + 3 Na]$^{4+}$, 1283.2 [M + 3 H]$^{3+}$. Elemental analysis calculated (%) for $C_{161}H_{315}Cl_{14}N_{35}O_{42}S_{14}$: C 44.36, H 7.28, N 11.25, S 10.30; found: C 44.54, H 7.44, N 11.36, S 10.55.

Acknowledgements

This work was supported by the Spanish Ministerio de Economia y Competitividad (MinECo, contract no. SAF2013-44021-R), the Junta de Andalucía (contract no. FQM2012-1467), the European Union (FEDER and FSE), the CSIC, the CNRS, and FUSINT (CNR project). We also thank the CITIUS for technical support. I. P. is grateful to CSIC (JAE-PreDoc program) for a predoctoral fellowship.

References

1 D. W. Pack, A. S. Hoffman, S. Pun and P. S. Stayton, *Nat. Rev. Drug Discovery*, 2005, **4**, 581.
2 Y. Zhang, A. Satterlee and L. Huang, *Mol. Ther.*, 2012, **20**, 1298.
3 H. Yin, R. L. Kanasty, A. A. Eltoukhy, A. J. Vegas, J. R. Dorkin and D. G. Anderson, *Nat. Rev. Genet.*, 2014, **12**, 541.
4 S. L. Ginn, I. E. Alexander, M. L. Edelstein, M. R. Abedi and J. Wixon, *J. Genet. Med.*, 2013, **15**, 65.
5 T. Wang, J. R. Upponi and V. P. Torchilin, *Int. J. Pharm.*, 2012, **427**, 3.
6 C. H. Jones, C.-K. Chen, A. Ravikrishnan, S. Rane and B. A. Pfeifer, *Mol. Pharmaceutics*, 2013, **10**, 4082.
7 E. V. B. van Gaal, R. Van Eijk, R. S. Oosting, R. J. Kok, W. E. Hennink, D. J. Crommelin and E. Mastrobattista, *J. Controlled Release*, 2011, **154**, 218.
8 T. M. Allen and P. R. Cullis, *Adv. Drug Delivery Rev.*, 2013, **65**, 36.
9 M. A. Kay, *Nat. Rev. Genet.*, 2011, **12**, 316.
10 Y. Ma, R. J. M. Nolte and J. J. M. L. Cornelissen, *Adv. Drug Delivery Rev.*, 2012, **64**, 811.
11 M. A. Mintzer and E. E. Simanek, *Chem. Rev.*, 2009, **109**, 259.
12 V. A. Bloomfield, *Biopolymers*, 1997, **44**, 269.
13 N. M. Rao, *Chem. Phys. Lipids*, 2010, **163**, 245.
14 R. N. Cohen, M. A. E. M. van der Aa, N. Macaraeg, A. P. Lee and F. C. Szoka, *J. Controlled Release*, 2009, **135**, 166.
15 D. V. Schaffer, N. A. Fidelman, N. Dan and D. A. Lauffenburger, *Biotechnol. Bioeng.*, 2000, **67**, 598.
16 C. L. Grigsby and K. W. Leong, *J. R. Soc., Interface*, 2010, **7**, s67.
17 Y. J. Kwon, *Acc. Chem. Res.*, 2012, **45**, 1077.
18 M. Köping-Höggård, K. M. Vårum, M. Issa, S. Danielsen, B. E. Christensen, B. T. Stokke and P. Artursson, *Gene Ther.*, 2004, **11**, 1441.
19 Y. Gao, Q. Yin, L. Chen, Z. Zhang and Y. Li, *Bioconjugate Chem.*, 2011, **22**, 1153.
20 M. X. Tang, C. T. Redemann and F. C. Szoka Jr., *Bioconjugate Chem.*, 1996, **7**, 703.
21 B. Wang, C. He, C. Tang and C. Yin, *Biomaterials*, 2011, **32**, 4630.
22 J. J. Green, R. Langer and D. G. Anderson, *Acc. Chem. Res.*, 2008, **41**, 749.
23 L. Xue, N. P. Ingle and T. M. Reineke, *Biomacromolecules*, 2013, **14**, 3903.
24 D. He and E. Wagner, *Macromol. Biosci.*, 2015, **15**, 600.
25 (*a*) R. Duncan, *Nat. Rev. Drug Discovery*, 2003, **2**, 347; (*b*) M. Baalousha and T. R. Lead, *Nat. Nanotechnol.*, 2013, **8**, 308.
26 (*a*) K. Ariga, J. Li, J. Fei, Q. Ji and J. P. Hill, *Adv. Mater.*, 2016, **28**, 1251; (*b*) K. Liu, R. Xing, Q. Zou, G. Ma, H. Möhwald and X. Yan, *Angew. Chem., Int. Ed.*, 2016, **55**, 3036; (*c*) C. Ortiz Mellet, J. M. Benito and J. M. García Fernández, *Chem. – Eur. J.*, 2010, **16**, 6728.

27 D. Sigwalt, M. Holler, J. Iehl, J.-F. Nierengarten, M. Nothisen, E. Morin and J.-S. Remy, *Chem. Commun.*, 2011, **47**, 4640.

28 M. Giuliani, I. Morbioli, F. Sansone and A. Casnati, *Chem. Commun.*, 2015, **51**, 14140.

29 R. V. Rodik, A.-S. Anthony, V. I. Kalchenko, Y. Mély and A. S. Klymchenko, *New J. Chem.*, 2015, **39**, 1654.

30 Y. Chang, K. Yang, P. Wei, S. Huang, Y. Pei, W. Zhao and Z. Pei, *Angew. Chem., Int. Ed.*, 2014, **53**, 13126.

31 E. Bartolami, Y. Bessin, V. Gervais, P. Dumy and S. Ulrich, *Angew. Chem., Int. Ed.*, 2015, **54**, 10183.

32 (*a*) C. Ortiz Mellet, J. M. García Fernández and J. M. Benito, *Chem. Soc. Rev.*, 2011, **40**, 1586; (*b*) J. Zhang and P. X. Ma, *Adv. Drug Delivery Rev.*, 2013, **65**, 1215.

33 A. Díaz-Moscoso, L. Le Gourriérec, M. Gómez-García, J. M. Benito, P. Balbuena, F. Ortega-Caballero, N. Guilloteau, C. Di Giorgio, P. Vierling, J. Defaye, C. Ortiz Mellet and J. M. García Fernández, *Chem. – Eur. J.*, 2009, **15**, 12871.

34 M. Gooding, M. Malhotra, D. J. McCarthy, B. M. D. C. Godinho, J. F. Cryan, R. Darcy and C. M. O'Driscoll, *Eur. J. Pharm. Sci.*, 2015, **71**, 80.

35 A. Méndez-Ardoy, K. Urbiola, C. Aranda, C. Ortiz Mellet, J. M. García-Fernández and C. Tros de Ilarduya, *Nanomedicine*, 2011, **6**, 1697.

36 B. M. Godinho, J. R. Ogier, A. Quinlan, R. Darcy, B. T. Griffin, J. F. Cryan and C. M. O'Driscoll, *Int. J. Pharm.*, 2014, **473**, 105.

37 V. Villari, A. Mazzaglia, R. Darcy, C. M. O'Driscoll and N. Micali, *Biomacromolecules*, 2013, **14**, 811.

38 (*a*) C. E. Nelson, J. R. Kintzing, A. Hanna, J. M. Shannon, M. K. Gupta and C. L. Duvall, *ACS Nano*, 2013, **7**, 8870; (*b*) R. Zhang, N. Zheng, Z. Song, L. Yin and J. Cheng, *Biomaterials*, 2014, **35**, 3443; (*c*) A. Dehshahri, R. K. Oskuee, W. T. Shier, A. Hatefi and M. Ramezani, *Biomaterials*, 2009, **30**, 4187; (*d*) W.-J. Yi, Q.-F. Zhang, J. Zhang, Q. Liu, L. Ren, Q.-M. Chen, L. Guo and X.-Q. Yu, *Acta Biomater.*, 2014, **10**, 1412.

39 (*a*) L. Gallego-Yerga, M. J. González-Álvarez, N. Mayordomo, F. Santoyo-González, J. M. Benito, C. Ortiz Mellet, F. Mendicuti and J. M. García Fernández, *Chem. – Eur. J.*, 2014, **20**, 6622; (*b*) L. Gallego-Yerga, L. Blanco-Fernández, K. Urbiola, T. Carmona, G. Marcelo, J. M. Benito, F. Mendicuti, C. Tros de Ilarduya, C. Ortiz Mellet and J. M. García Fernández, *Chem. – Eur. J.*, 2015, **21**, 12093.

40 A. Díaz-Moscoso, N. Guilloteau, C. Bienvenu, A. Méndez-Ardoy, J. L. Jiménez Blanco, J. M. Benito, L. Le Gourriérec, C. Di Giorgio, P. Vierling, J. Defaye, C. Ortiz Mellet and J. M. García Fernández, *Biomaterials*, 2011, **32**, 7263.

41 J. L. Jiménez Blanco, F. Ortega-Caballero, C. Ortiz Mellet and J. M. García Fernández, *Beilstein J. Org. Chem.*, 2010, **6**, 20.

42 A. Gadelle and J. Defaye, *Angew. Chem., Int. Ed.*, 1991, **30**, 78.

43 D. M. Kneeland, K. Ariga, V. M. Lynch, C. Y. Huang and E. V. Anslyn, *J. Am. Chem. Soc.*, 1993, **115**, 10042.

44 A. Díaz-Moscoso, A. Méndez-Ardoy, F. Ortega-Caballero, J. M. Benito, C. Ortiz Mellet, J. Defaye, T. M. Robinson, A. Yohannes, K. A. Karginov and J. M. García Fernández, *ChemMedChem*, 2011, **6**, 181.

45 S. Srinivasachari, K. M. Fichter and T. M. Reineke, *J. Am. Chem. Soc.*, 2008, **130**, 4618.

46 J. M. Layman, S. M. Ramirez, M. D. Green and T. E. Long, *Biomacromolecules*, 2009, **10**, 1244.

47 Y. Shen, J. Wang, Y. Li, Y. Tian, H. Sun, O. Ammar, J. Tu, B. Wang and C. Sun, *RSC Adv.*, 2015, **5**, 46464.

48 N. Symens, A. Méndez-Ardoy, A. Díaz-Moscoso, E. Sánchez-Fernández, K. Remaut, J. Demeester, J. M. García Fernández, S. C. De Smedt and J. Rejman, *Bioconjugate Chem.*, 2012, **23**, 1276.

49 O. Boussif, F. Lezoualc'h, M. A. Zanta, M. D. Mergny, D. Scherman, B. Demeneix and J.-P. Behr, *Proc. Natl. Acad. Sci. U. S. A.*, 1995, **92**, 7297.

50 A. Díaz-Moscoso, D. Vercauteren, J. Rejman, J. M. Benito, C. Ortiz Mellet, S. C. De Smedt and J. M. García Fernández, *J. Controlled Release*, 2010, **143**, 318.

51 J. Gaucheron, C. Boulanger, C. Santaella, N. Sbirrazzouli, O. Boussif and P. Vierling, *Bioconjugate Chem.*, 2001, **12**, 949.